PHILOSOPHICAL TRANSACTIONS OF THE ROYAL SOCIETY A

Phil. Trans. R. Soc. A (2009) **367**, 1445–1486
doi:10.1098/rsta.2009.0011
Published online

Introduction

Biomimetics: lessons from nature – an overview

By Bharat Bhushan*

Nanoprobe Laboratory for Bio- & Nanotechnology and Biomimetics, Ohio State University, 201 West 19th Avenue, Columbus, OH 43210-1142, USA

Nature has developed materials, objects and processes that function from the macroscale to the nanoscale. These have gone through evolution over 3.8 Gyr. The emerging field of biomimetics allows one to mimic biology or nature to develop nanomaterials, nanodevices and processes. Properties of biological materials and surfaces result from a complex interplay between surface morphology and physical and chemical properties. Hierarchical structures with dimensions of features ranging from the macroscale to the nanoscale are extremely common in nature to provide properties of interest. Molecular-scale devices, superhydrophobicity, self-cleaning, drag reduction in fluid flow, energy conversion and conservation, high adhesion, reversible adhesion, aerodynamic lift, materials and fibres with high mechanical strength, biological self-assembly, antireflection, structural coloration, thermal insulation, self-healing and sensory-aid mechanisms are some of the examples found in nature that are of commercial interest. This paper provides a broad overview of the various objects and processes of interest found in nature and applications under development or available in the marketplace.

Keywords: biomimetics; bionics; biomimicry; biognosis; lessons from nature; nanotechnology

1. Introduction

Nature has gone through evolution over the 3.8 Gyr since life is estimated to have appeared on the Earth (Gordon 1976). Nature has evolved objects with high performance using commonly found materials. These function on the macroscale to the nanoscale. The understanding of the functions provided by objects and processes found in nature can guide us to imitate and produce nanomaterials, nanodevices and processes. Biologically inspired design or adaptation or derivation from nature is referred to as 'biomimetics'. It means mimicking biology or nature. Biomimetics is derived from the Greek word biomimesis. The word was coined by polymath Otto Schmitt in 1957, who, in his doctoral research, developed a physical device that mimicked the electrical action of a nerve. Other words used include bionics (coined in 1960 by Jack Steele of

*bhushan.2@osu.edu

One contribution of 9 to a Theme Issue 'Biomimetics I: functional biosurfaces'.

Wright-Patterson Air Force Base in Dayton, OH), biomimicry and biognosis. The field of biomimetics is highly interdisciplinary. It involves the understanding of biological functions, structures and principles of various objects found in nature by biologists, physicists, chemists and material scientists, and the design and fabrication of various materials and devices of commercial interest by engineers, material scientists, chemists and others. The word biomimetics first appeared in Webster's dictionary in 1974 and is defined as 'the study of the formation, structure or function of biologically produced substances and materials (as enzymes or silk) and biological mechanisms and processes (as protein synthesis or photosynthesis) especially for the purpose of synthesizing similar products by artificial mechanisms which mimic natural ones'.

Biological materials are highly organized from the molecular to the nanoscale, microscale and macroscale, often in a hierarchical manner with intricate nanoarchitecture that ultimately makes up a myriad of different functional elements (Alberts *et al.* 2008). Nature uses commonly found materials. Properties of the materials and surfaces result from a complex interplay between the surface structure and the morphology and physical and chemical properties. Many materials, surfaces and devices provide multifunctionality. Molecular-scale devices, superhydrophobicity, self-cleaning, drag reduction in fluid flow, energy conversion and conservation, high adhesion, reversible adhesion, aerodynamic lift, materials and fibres with high mechanical strength, biological self-assembly, antireflection, structural coloration, thermal insulation, self-healing and sensory-aid mechanisms are some of the examples found in nature that are of commercial interest.

(*a*) *Industrial significance*

The word biomimetics is relatively new; however, our ancestors looked to nature for inspiration and development of various materials and devices many centuries ago (Ball 2002; Bar-Cohen 2006; Vincent *et al.* 2006; Anon. 2007; Meyers *et al.* 2008). For example, the Chinese tried to make artificial silk some 3000 years ago. Leonardo da Vinci, a genius of his time, studied how birds fly and proposed designs of flying machines. In the twentieth century, various products, including the design of aircraft, have been inspired by nature. Since the 1980s, the artificial intelligence and neural networks in information technology have been inspired by the desire to mimic the human brain. The existence of biocells and DNA serves as a source of inspiration for nanotechnologists, who hope to one day build self-assembled molecular-scale devices. In molecular biomimetics, proteins are being used to control materials formation in practical engineering towards self-assembled, hybrid, functional materials structure (Grunwald *et al.* in press; Sarikaya & Tamerler in press). Since the mid-1990s, the so-called lotus effect has been used to develop a variety of surfaces for superhydrophobicity, self-cleaning, drag reduction in fluid flow and low adhesion (Bhushan *et al.* in press). Replication of the dynamic climbing and peeling ability of geckos has been carried out to develop treads of wall-climbing robots (Cutkosky & Kim in press). Replication of shark skin has been used to develop moving objects with low drag, e.g. whole body swimsuits. Nanoscale architecture used in nature for optical reflection and antireflection has been used to develop reflecting and antireflecting surfaces. In the field of biomimetic

materials, there is an area of bioinspired ceramics based on seashells and other biomimetic materials. Inspired by furs of the polar bear, artificial furs and textiles have been developed. Self-healing of biological systems found in nature is of interest for self-repair. Biomimetics is also guiding in the development of sensory-aid devices.

Various features found in nature's objects are on the nanoscale. The major emphasis on nanoscience and nanotechnology since the early 1990s has provided a significant impetus in mimicking nature using nanofabrication techniques for commercial applications (Bhushan 2007*a*). Biomimetics has spurred interest across many disciplines.

It is estimated that the 100 largest biomimetic products had generated approximately US $1.5 billion over 2005–2008. The annual sales are expected to continue to increase dramatically.

(*b*) *Objective*

The objective of this paper is to provide a broad overview of the field of biomimetics. It will provide a description of objects and processes of interest found in nature and applications under development or available in the marketplace. The paper will end with an outlook of the field.

2. Lessons from nature and applications

There are a large number of objects, including bacteria, plants, land and aquatic animals and seashells, with properties of commercial interest. Figure 1 provides an overview of various objects from nature and their selected functions, whose detailed descriptions follow. Figure 2 shows a montage of some examples from nature. These serve as the inspiration for various technological developments.

(*a*) *Bacteria*

The flagella of bacteria rotate at over 10 000 r.p.m. (Jones & Aizawa 1991). This is an example of a biological molecular machine. The flagella motor is driven by the proton flow caused by the electrochemical potential differences across the membrane. The diameter of the bearing is approximately 20–30 nm, with an estimated clearance of approximately 1 nm.

(*b*) *Plants*

(i) *Chemical energy conversion*

Several billion years ago, molecules began organizing into complex structures that could support life. Photosynthesis harnesses solar energy to support plant life. Molecular ensembles present in plant leaves, which include light-harvesting molecules such as chlorophyll (green pigment) arranged within the cells (on the nanometre to micrometre scales), capture light energy and convert it into the chemical energy that drives the biochemical machinery of plant cells. Live organs use chemical energy in the body. This technology is being exploited to develop dye-sensitized polymer-based solar cells by various industries such as Konarka

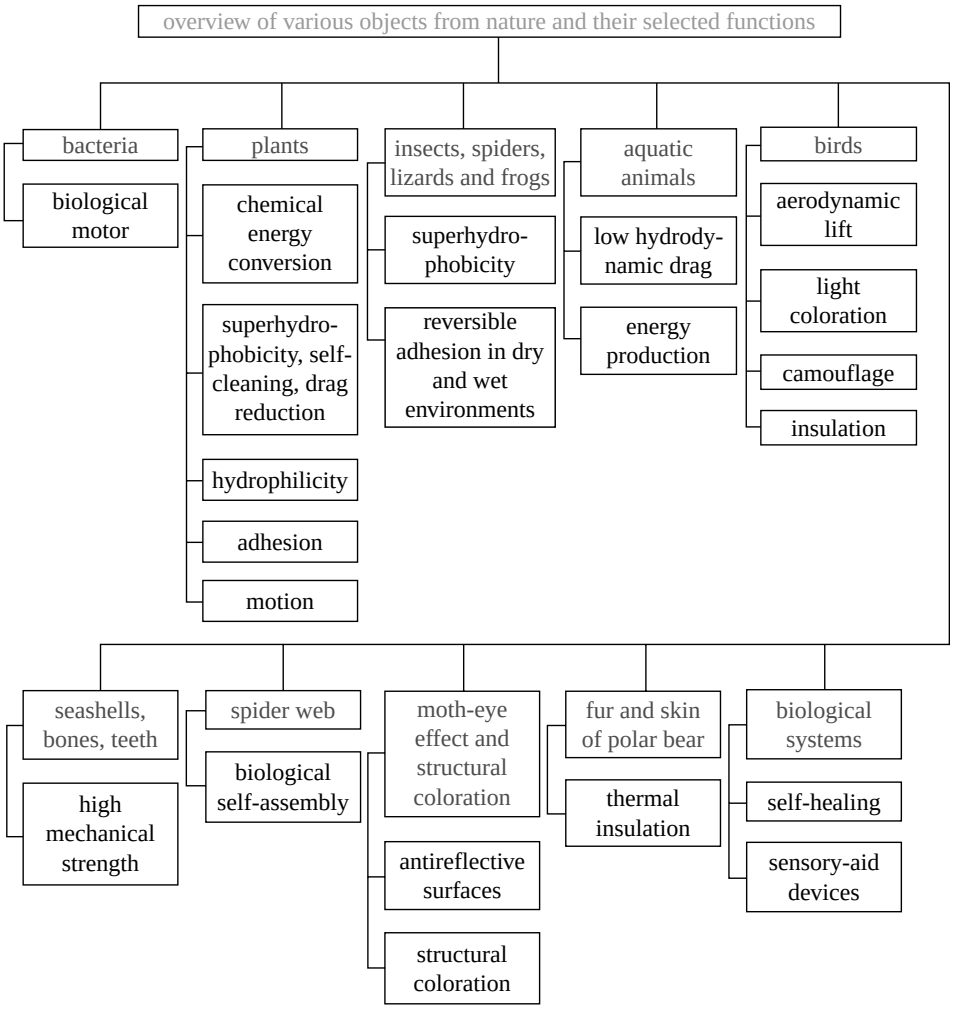

Figure 1. An overview of various objects from nature and their selected functions.

Technologies in the USA and Dyesol in Australia (Benniston & Harriman 2008). These cells are not as efficient as photovoltaics, in which solar photovoltaic arrays (solar cells) are used to convert energy from the Sun into electricity, but they are significantly cheaper and more flexible.

(ii) *Multifunctional properties and surface structures of plant leaves*

Diversity in the structure and morphology of plant leaf surfaces provides multifunctional properties (Koch *et al.* 2008, 2009, in press *a*). The outermost layer of the primary plant surface is known as the cuticle, and its most prominent functions are presented in figure 3. One of the most important attributes of the cuticle is its hydrophobicity that enables plants to overcome the physical and physiological problems connected to an ambient environment, such as desiccation. The cuticle also stabilizes the plant tissue and has several protective

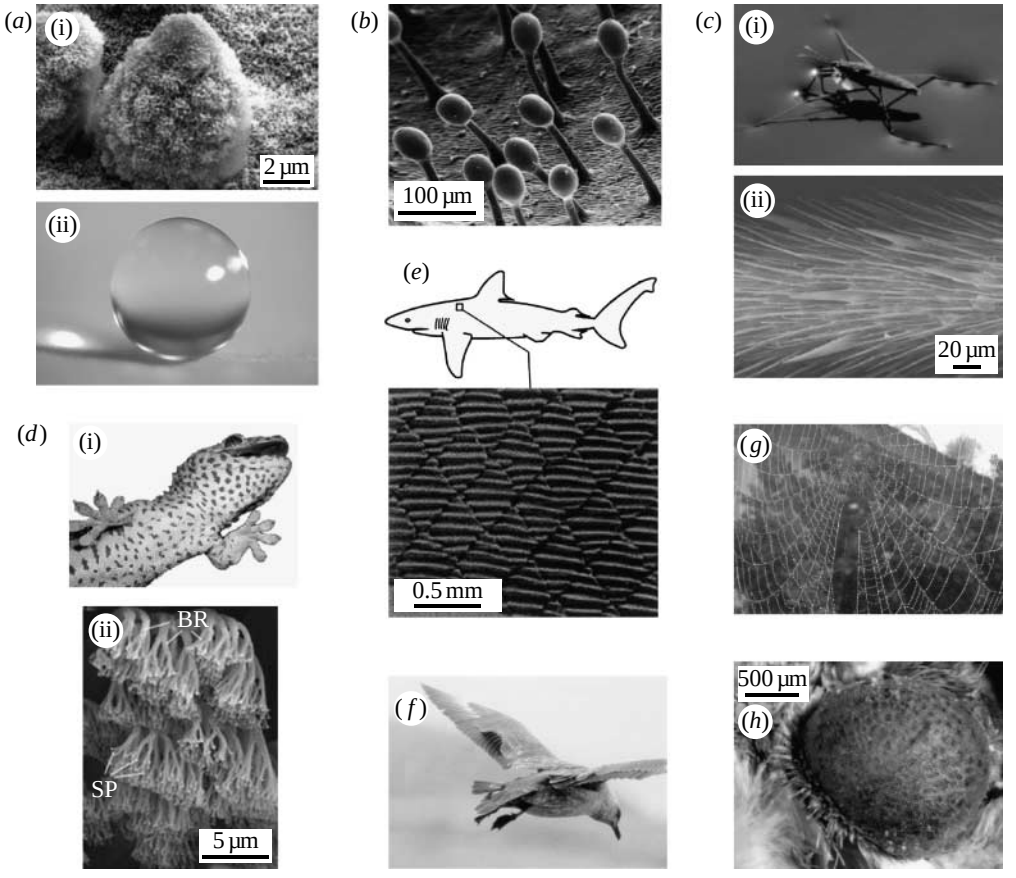

Figure 2. Montage of some examples from nature. (*a*) Lotus effect (Bhushan *et al.* in press), (*b*) glands of carnivorous plant secrete adhesive to trap insects (Koch *et al.* in press *c*), (*c*) pond skater walking on water (Gao & Jiang 2004), (*d*) gecko foot exhibiting reversible adhesion (Gao *et al.* 2005), (*e*) scale structure of shark reducing drag (Reif 1985), (*f*) wings of a bird in landing approach, (*g*) spiderweb made of silk material (Bar-Cohen 2006), and (*h*) antireflective moth's eye (Genzer & Efimenko 2006).

properties. One of the most important properties is the transpiration barrier function. This property is based on the material, made basically of a polymer called cutin and integrated and superimposed lipids called 'waxes', which are hydrophobic. In addition to the reduction of water loss, the cuticle prevents leaching of ions from inside the cells to the environment. In plants, a wide spectra of surface structures exist, which modify surface wettability and also have a significant influence on particle adhesion. Evolutionary optimized wettable or non-wettable surfaces can be found in water and wetland plants, e.g. the water-repellent leaves of lotus (*Nelumbo nucifera*). In submerged water growing plants and some tropical and subtropical plants, the cuticles provide hydrophilicity by providing a permanently wet surface or by water spreading, respectively. The plant cuticle also plays an important role for insect and micro-organism interaction. In some cases, it protects the plants against overheating by reflecting radiation and/or by heat transfer via turbulent airflow and convection.

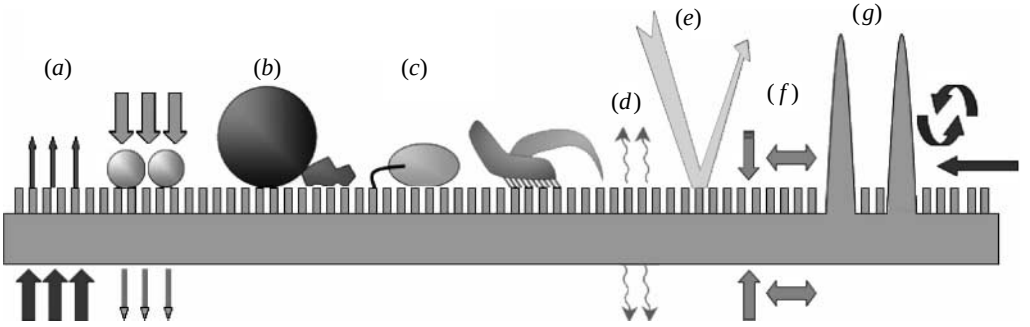

Figure 3. Schematic of the most prominent functions of the boundary layer on a hydrophobic microstructured plant surface. (*a*) Transport barrier limitation of uncontrolled water loss/leaching from interior and foliar uptake, (*b*) surface wettability, (*c*) anti-adhesive, self-cleaning properties: reduction of contamination, pathogen attack and reduction of attachment/locomotion of insects, (*d*) signalling: cues for host–pathogens/insect recognition and epidermal cell development, (*e*) optical properties: protection against harmful radiation, (*f*) mechanical properties: resistance against mechanical stress and maintenance of physiological integrity, and (*g*) reduction of surface temperature by increasing turbulent air flow over the boundary air later (Koch *et al.* 2009).

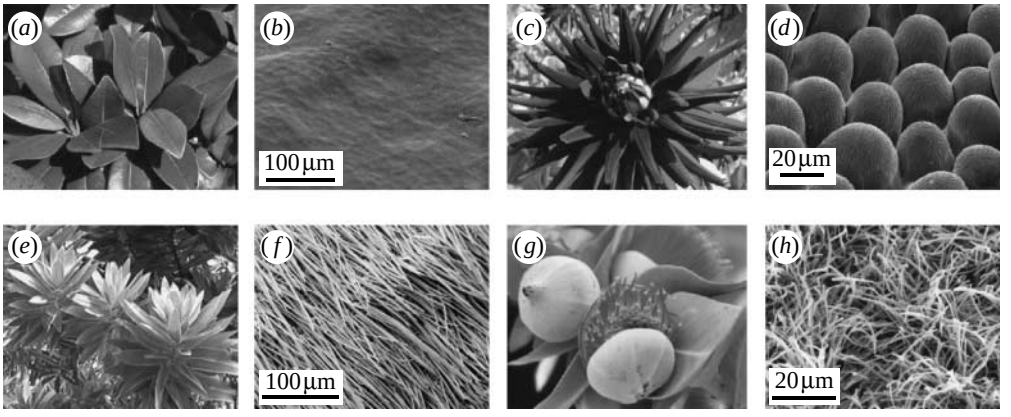

Figure 4. Macroscopically visible optical appearance of plant surfaces and their surface microstructures, shown in scanning electron microscope (SEM) micrographs. In (*a*) leaves (*Magnolia grandiflora*) appear glossy because of the flat surface structure of the surface, shown in (*b*). In (*c*) the flower leaves (*Dahlia*) appear velvety, because of the microstructure of the epidermal cells shown in (*d*). In (*e*) the white appearance of the leaves (*Leucadendron argenteum*) is caused by a dense layer of hairs, shown in (*f*). (*g*) A white or bluish leaf surface (*Eucalyptus macrocarpa*) that is densely covered with three-dimensional waxes shown in (*h*) (Koch *et al.* 2009).

The micro- and nanostructures of plant surfaces have a great influence on their attributes as interfaces. Even in a cursory look at different plant surfaces, they show different optical appearances, which arise from the surface structures in the micro- and nanoscale dimension (Koch *et al.* 2009). The optical appearance of selected plant surfaces and their surface microstructures are shown in figure 4. Based on their microscopically smooth surface, the leaves of *Magnolia grandiflora* appear glossy (figure 4*a*,*b*), whereas the rougher surfaces of the flower leaves (petals) of *Dahlia* appear velvety and soft (figure 4*c*,*d*). The leaves

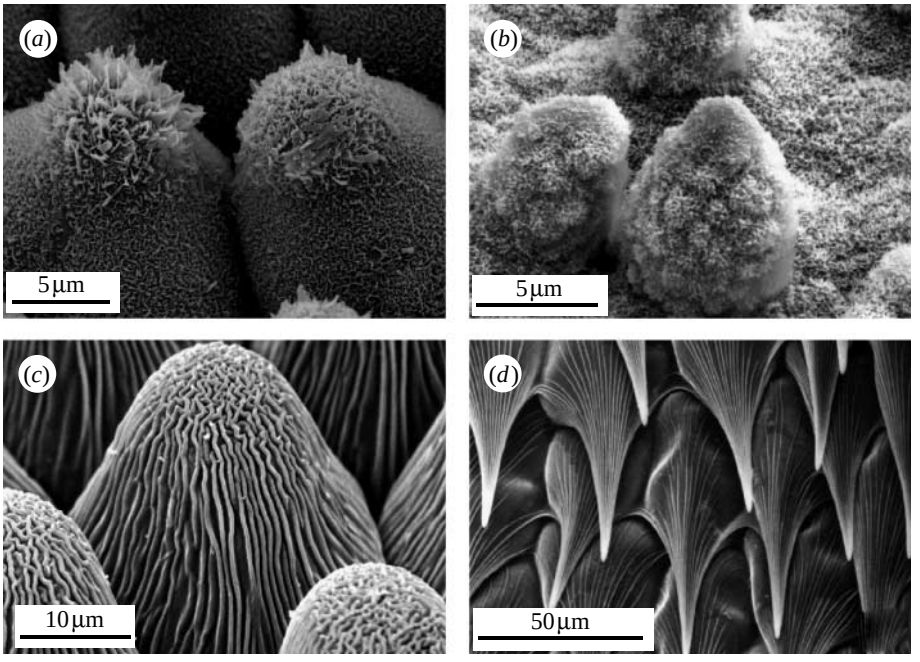

Figure 5. SEM micrographs of hierarchical structures on plant surfaces. (*a*,*b*) Double structured plant surfaces with convex cell shapes and superimposed three-dimensional epicuticular waxes on the upper (adaxial) leaf sides of (*a*) *Colocasia esculenta* and (*b*) *N. nucifera*. (*c*,*d*) Convex cells with cuticular folding. (*c*) The flower leaf of *Rosa montana* (adaxial side) with a rippled folded cuticle in the central field of the cells and parallel folding. (*d*) The cells of the inner side of a tube-like leaf of the carnivorous plant *Sarracenia leucophylla*. These cells are downward trending hair papilla with a parallel cuticle folding (Koch *et al.* 2008).

of *Leucadendron argenteum* appear white because of a dense layer of air-filled hollow hairs (figure 4*e*,*f*). The leaves of *Eucalyptus macrocarpa* appear bluish due to a coverage of three-dimensional waxes (figure 4*g*,*h*). The leaves in figure 4*a*–*d* are hydrophilic and in figure 4*g*,*h* are superhydrophobic. The great diversity in surface structures originates from the diversity of species, combined with the different structures found in a single plant. Today, plant biodiversity contains approximately 270 000 different species, but recent calculations suggest that most species on the Earth have not yet been described and will not be because of the high rates of species extinction (50 per day; Koch *et al.* 2008).

Hierarchical structure is found on a large number of plant surfaces and is of much interest to provide a large range of properties that are desirable for a given object (Koch *et al.* 2008). Both the three-dimensional epicuticular waxes and cuticular folding are able to create the double structure. In figure 5*a*,*b*, examples are characterized by papilla and convex cells with three-dimensional waxes on top. In *Colocasia esculenta* (figure 5*a*) the wax crystals are wax platelets, whereas the waxes of *N. nucifera* (figure 5*b*) are nonacosan-ol tubules. Figure 5*c*,*d* shows convex cells with cuticular folding. In a flower leaf of *Rosa Montana* (adaxial side), a rippled folded cuticle forms the central field of the cells, and parallel folds occur at the anticline field (figure 5*c*). Another example is the hair-papilla cells of the side of

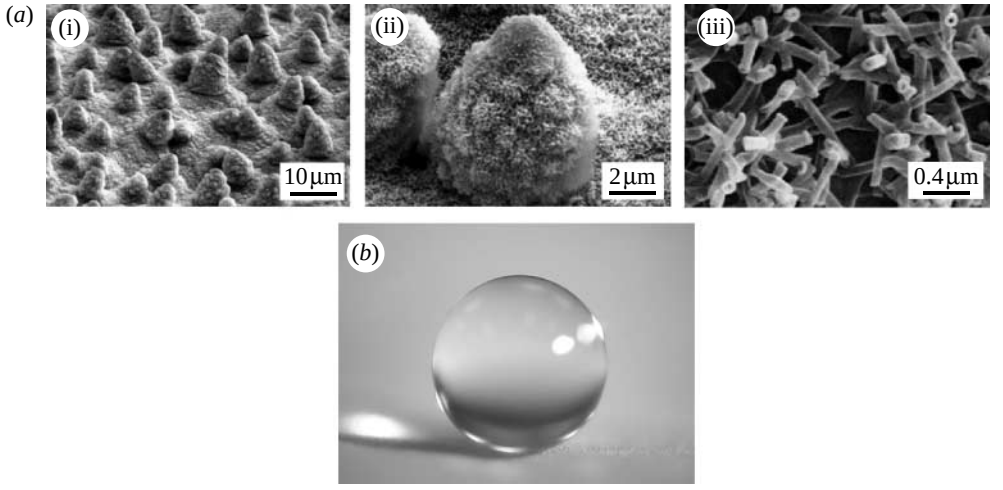

Figure 6. (*a*) SEM micrographs (shown at three magnifications) of lotus (*N. nucifera*) leaf surface, which consists of microstructure formed by papillose epidermal cells covered with epicuticular wax tubules on the surface, which create nanostructure (Bhushan *et al.* in press) and (*b*) image of water droplet sitting on the lotus leaf.

the tube-like leaf of the carnivorous plant *Sarracenia leucophylla* (figure 5*d*). The cells are downward trending hair papilla with a parallel cuticle folding, with larger distances at the bases and denser arrangements at the cell tip.

Superhydrophobicity, self-cleaning and low adhesion

Some leaves of water-repellent plants, such as *N. nucifera* (lotus) and *C. esculenta*, are known to be superhydrophobic and self-cleaning due to hierarchical roughness (microbumps superimposed with nanostructure) and the presence of a hydrophobic coating (Bhushan & Jung 2008; Koch *et al.* 2008, 2009, in press *a*; Nosonovsky & Bhushan 2008*a–c*). Roughness-induced superhydrophobic and self-cleaning surfaces are of interest in various applications, including self-cleaning windows, windshields and exterior paints for buildings, boats, ships and aircraft, utensils, roof tiles, textiles, solar panels and applications requiring antifouling and a reduction of drag in fluid flow, e.g. in micro/nanofluidics, boats, ships and aircraft. Superhydrophobic surfaces can also be used for energy conversion and conservation. Non-wetting surfaces also reduce stiction at a contacting interface in machinery (Bhushan 1999, 2002).

Surfaces are called hydrophobic if the static contact angle is greater than 90°. Surfaces are called superhydrophobic if the static contact angle is above 150°. In addition, a low contact angle hysteresis (CAH; the difference between the advancing and receding contact angles) plays an important role in self-cleaning and reduction of drag in fluid flow. The CAH is a measure of energy dissipation during the flow of a droplet along a solid surface. At a low value of CAH, the droplet may roll in addition to slide, which facilitates the removal of contaminant particles. A CAH of less than 10° is generally referred to as a self-cleaning surface. Surfaces with low CAH have a low water roll-off (tilt) angle, which denotes the angle to which a surface must be tilted for roll-off of water drops.

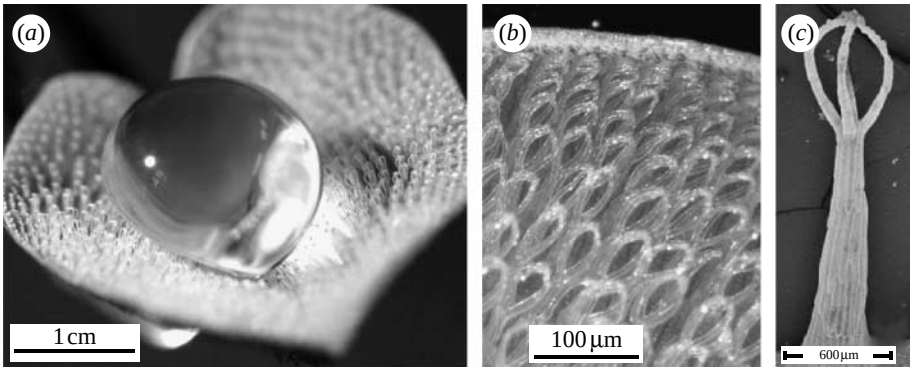

Figure 7. Hairs on the leaves of the water fern genus *Salvinia* are multicellular surface structures. In (*a*) a water droplet on the upper leaf side of *Salvinia biloba* is shown. (*b*,*c*) The crown-like morphology of the hairs of *S. biloba* (Koch *et al.* 2009).

A model surface for superhydrophobicity and self-cleaning is provided by the leaves of the lotus plant (*N. nucifera*; figure 6*a*; Barthlott & Neinhuis 1997; Neinhuis & Barthlott 1997; Wagner *et al.* 2003; Bhushan & Jung 2006; Koch *et al.* 2008, 2009, in press *a*). The so-called papillose epidermal cells form asperities or papillae and provide roughness on the microscale. The surface of the leaves is usually covered with a range of waxes made from a mixture of long-chain hydrocarbon compounds that have a strong phobia of being wet. Submicrometre-sized asperities composed of the three-dimensional epicuticular waxes are superimposed over microscale roughness, creating a hierarchical structure. The wax asperities consist of different morphologies, such as tubules on lotus or platelets on Colocasia (Koch *et al.* 2008, 2009, in press *a*). The water droplets on these surfaces readily sit on the apex of nanostructures because air bubbles fill in the valleys of the structure under the droplet. Therefore, these leaves exhibit considerable superhydrophobicity (figure 6*b*). The water droplets on the leaves remove any contaminant particles from their surfaces when they roll off, leading to self-cleaning. A contact angle of 164° and a CAH of 3° have been reported for the lotus leaf (Bhushan *et al.* in press; Koch *et al.* in press *b*).

Another example of superhydrophobic leaves is floating water ferns. Within the floating water ferns of the genus *Salvinia*, morphologically different kinds of water-repellent (superhydrophobic) hairs exist (Koch *et al.* 2009). Depending on the species, the hair size varies of the order of several hundreds of micrometres, and hairs are visible with the naked eye (figure 7*a*). These multicellular hairs on the upper (adaxial) side of the leaves form complex hierarchical surface structures that are able to retain an air layer at the surface, even when the leaves were fixed under water for several days. The hairs have the shape of tiny crowns (figure 7*b*,*c*).

Formation of composite solid–air–liquid surfaces is critical to superhydrophobicity and self-cleaning. Surface roughness on a hydrophilic or hydrophobic surface decreases or increases the contact angle, respectively, based on the so-called Wenzel effect. Air pocket formation in the valleys can increase the contact angle for both hydrophilic and hydrophobic surfaces based on the so-called Cassie–Baxter effect (Bhushan & Jung 2008). Formation of air pockets, leading to a composite interface, is the key to very high contact angle and

low CAH. Nosonovsky & Bhushan (2008*a–c*) reported that the composite interface is metastable. Capillary waves may destabilize the composite interface. Condensation and accumulation of nanodroplets and surface inhomogeneity (with hydrophobic spots) may destroy the composite interface. Microstructures resist capillary waves present at the liquid–air interface. Nanostructure prevents nanodroplets from filling the valleys between asperities and pin the droplet. Thus, a hierarchical structure is required to resist these scale-dependent mechanisms and enlarge the liquid–air interface, resulting in a high static contact angle and low CAH. It has been reported that all superhydrophobic and self-cleaning leaves consist of an intrinsic hierarchical structure (Barthlott & Neinhuis 1997; Neinhuis & Barthlott 1997; Koch *et al.* 2008, 2009, in press *a*).

Based on this lesson from nature, one of the ways to increase the hydrophobic property of the surface is to increase surface roughness; so roughness-induced hydrophobicity has become a subject of extensive investigations. This understanding also allows us to develop superoleophobic surfaces (which repel low surface tension liquids). This technology is being used to develop various products.

Various superhydrophobic surfaces have been either produced in the laboratory or are produced commercially (Bhushan *et al.* in press; Koch *et al.* in press *b*; Roach *et al.* 2008). Self-cleaning paints, roof tiles, fabrics and glass windows are commercially available. Some paints have been formulated to keep barnacles from sticking to ship hulls. An exterior self-cleaning paint (Sto, AG) is sold under the trade name Lotusan (Dendl & Interwies 2001). It consists of particles with a controlled size to provide surface structure. A hydrophobic titanium oxide is subsequently applied. Self-cleaning coatings for glassware, vehicles, lighting and optical sensors have been developed by the company Ferro, which are transparent and permanent (Baumann *et al.* 2003). These coatings contain functional pigments, nanoparticles and binders in a liquid medium. During firing after application, a special micro- and nanostructured surface is formed. Removable coatings with a dispersion of nanoparticles are available from Evonik Degussa, Inc., which can be removed at a later time, if needed (Mueller & Winter 2004). Clothes can be waterproofed using plasma treatment (Hoecker 2002). Various coatings with nanostructured particles are available, which can be applied to textiles to make them hydrophobic and self-cleaning (Nun *et al.* 2002; Gao & McCarthy 2006).

Surfaces that switch between superhydrophobicity and hydrophilicity have been developed using, for example, photoresponsive surfaces with inorganic oxides and photoreactive organic molecules (Wang *et al.* 2007), copolymer films sensitive to pH (Xia *et al.* 2006) or electric field (electrowetting; Bhushan & Ling 2008). These surfaces can be used, for example, to control fluid flow in micro/nanochannel networks in micro/nanofluidic chips.

Hydrophilicity

Some plant leaves are hydrophilic or superhydrophilic (Koch *et al.* 2008, 2009, in press *a*). Surfaces are called superhydrophilic if the contact angle is below 10°. Plant surfaces can either absorb water or let water spread over its surface. Two leaves with water-absorbing porous surface structures are shown in figure 8.

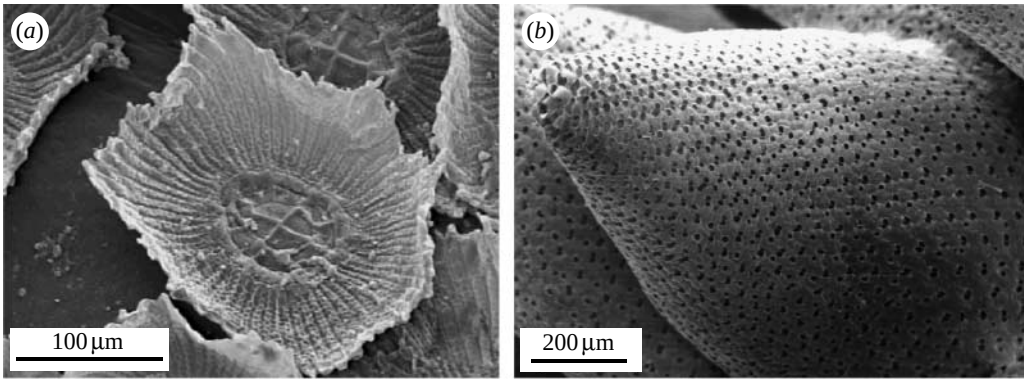

Figure 8. SEM micrographs of superhydrophilic plant surfaces showing (*a*) water-absorbing hair structure of *Tillandsia usneoides* and (*b*) the water uptaking pores of *Sphagnum* moss (Koch *et al.* 2008).

A contact angle of the order of 0° is expected of these plant surfaces because they are water absorbing. The structure of these plant surfaces can be used in the development of adhesive or sticky surfaces.

Insect feeding

Two strategies used for catching insects by plants for digestion are having sticky surfaces or sliding structures. As an example, for catching insects using sticky surfaces, the glands of the carnivorous plants of the genus *Pinguicula* (butterworts) and *Drosera* (sundew), shown in figure 9, secrete adhesives and enzymes to trap and digest small insects, such as mosquitoes and fruit flies (Koch *et al.* 2009). In *Pinguicula*, the stalked glands are the sticky ones that trap the insects by secreting an adhesive solution. The shorter ones are those that secrete digestive enzymes, including protease and phosphotase, and later resorb the digested material. In *Drosera*, the stalked glands can effectively enclose small flies by bringing numerous glands in contact with the prey.

Some plants use slippery wax layers in order to capture and retain insects. Carnivorous plants in the genus *Nepenthes* have pitcher-like leaves formed as traps for catching and digestion of insects (figure 10*a–e*; Juniper *et al.* 1989; Koch *et al.* in press *a*). In these species, a layer of three-dimensional wax platelets creates a slippery zone inside the tube, above the digestive zone. The wax plays a crucial role in animal trapping and prey retention (Gorb *et al.* 2005). Insects are not able to attach and walk on these waxy surfaces. They glide into the digestive fluid and are restrained from further escape. The structure of these plant surfaces can be used in the development of surfaces with self-cleaning ability or for drag reduction.

Prevent feeding by insects

Some plants provide mechanical and chemical defence mechanisms to prevent feeding by insects. As an example for mechanical defence, for the surface of the common Horsetail (*Equisetum arvensis*), as shown in figure 11,

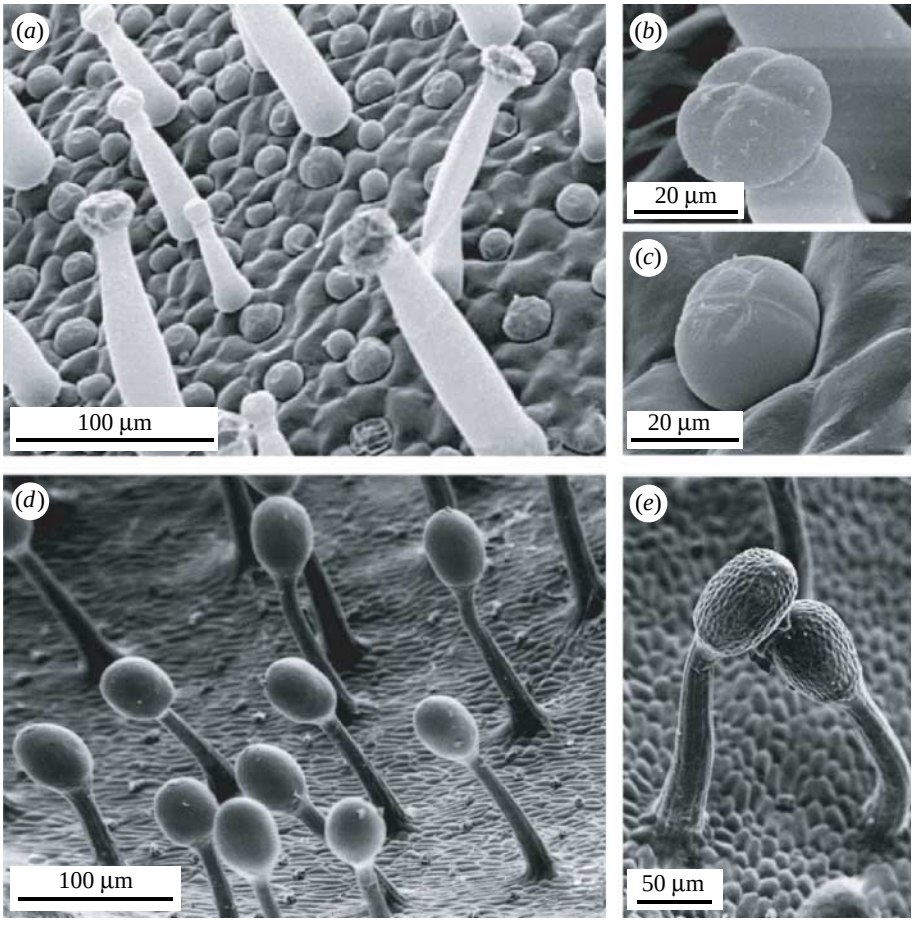

Figure 9. SEM micrographs of multicellular glands on plant surface. (*a*–*c*) Glands of the carnivorous plant *Pinguicula gypsicola* on the upper (adaxial) side of the leaf. (*b*) Detail of the stalked and (*c*) non-stalked glands. The stalked glands secrete an adhesive to trap small insects; unstalked glands provide the enzymes for digestion of the insects. (*d*,*e*) The sticky and also digestive glands of the carnivorous sundew (*Drosera capinsis*; Koch *et al.* 2009).

there are subcuticular inserts of solid crystals of silica. Silicon is a bioactive element associated with beneficial effects of mechanical and physiological properties of plants. Silicon enhances the expression of genetically controlled defence mechanisms in plants. This increases the resistance of plants to pathogenic fungi (Koch *et al.* 2008). These leaves are also an example of superhydrophobic surfaces.

Examples of plants that provide chemical defence include *Taxus baccata*, *Primula polinuri* and *Nicotiana tabacum* with exudates of glands—terpenoids, flavonoids and nicotine, respectively. The flavonoid exudates are morphologically similar to waxes, but are widely referred to as ‘farina’ or ‘farinose’ due to their chemical divergence to plant waxes (Koch *et al.* 2009).

Some of these defence strategies are of interest in the development of defence strategies against insect invasions of forests and in other applications.

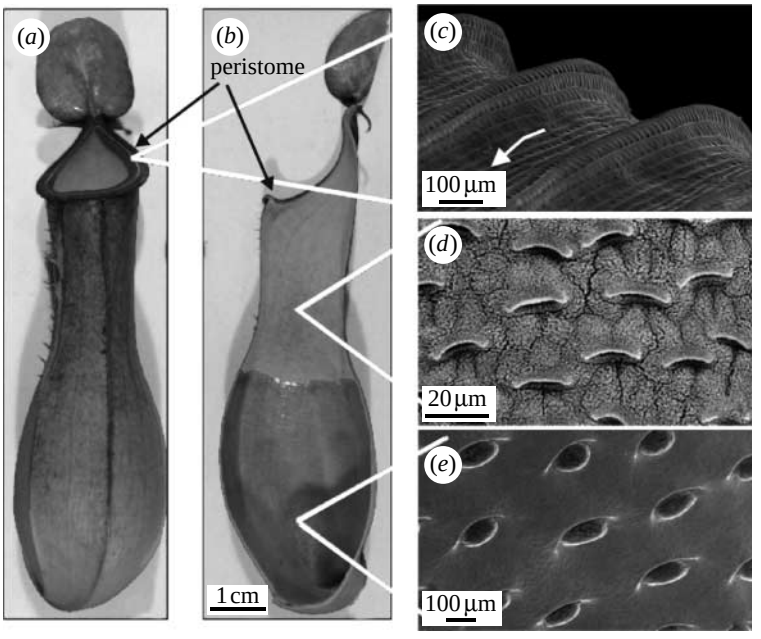

Figure 10. Pitcher traps of the carnivorous plant *Nepenthes alata*. (*a*) The complete pitcher trap of *N. alata* and (*b*) a longitudinal cut through the trap. (*c*) Parallel ridges of the hydrophilic peristome. The arrow indicates the direction towards the inside of the pitcher. (*d*) The waxy and slippery surface inside the trap, with inactive stomata. (*e*) Glands located in the digestive zone at the lower part of the trap. (*c*) was kindly provided by Holger Bohn (Koch *et al.* in press *a*).

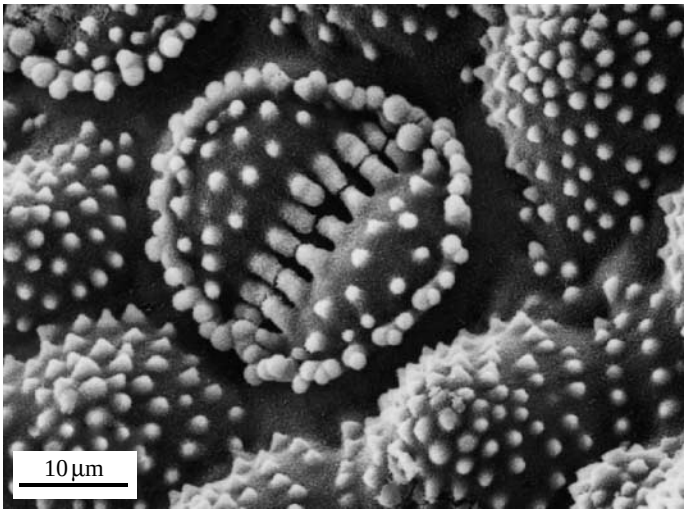

Figure 11. SEM micrograph of the cell surface structures of the common Horsetail (*E. arvensis*). In the middle of the figure, a stomata is shown. The stomatal cells and the surrounding cells are convex and have a micropattern of some small enhanced spots on the cells. The latter are formed by subcuticular inserts of bioactive silicon oxide crystals, which provide a defence mechanism. The surface consists of a three-dimensional wax layer producing a hierarchical structure (Koch *et al.* 2008).

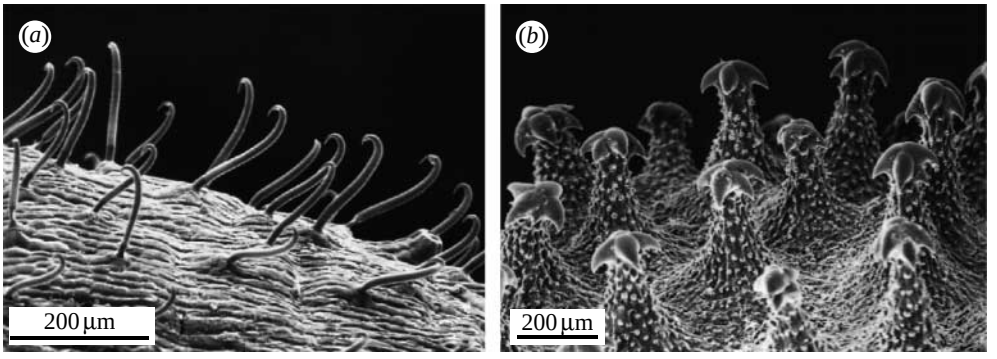

Figure 12. SEM micrographs of hairs; (*a*) the shoot surface of a climbing bean plant *P. vulgaris* with terminal hooks and (*b*) single hairs on a seed surface of *Cynoglossum officinale* are characterized by terminal and lateral barbed hooks for seed dispersal (Koch *et al.* 2009).

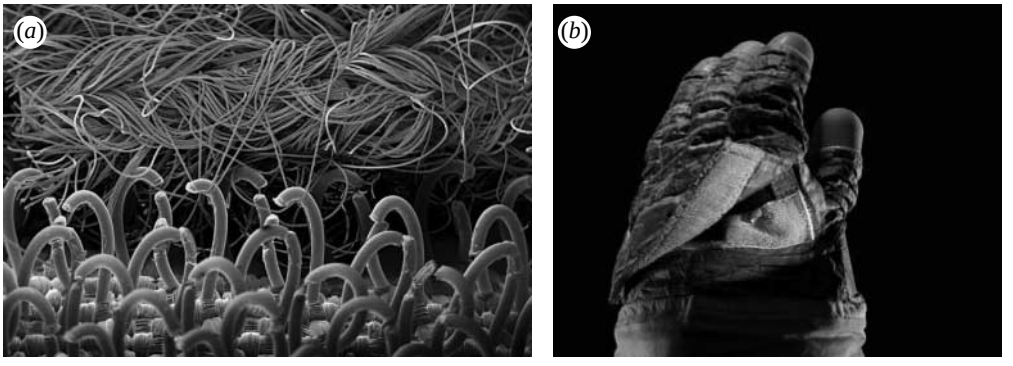

Figure 13. (*a*) The image of tiny hooks found in cockleburs and (*b*) a commercial Velcro (Mueller 2008).

Hair with hooks

Many plant surfaces have hairs (also known as trichomes). The hairs are found on the aerial surfaces of most flower plants, some conifers and mosses (Koch *et al.* 2009). The structures of these hairs are often complex. The function of the hairs varies from one plant to another (Wagner *et al.* 2004). Many plants of dry habitats show a dense cover of dead air-filled hairs to reflect visible light, which makes the surface appear white (figure 4*f*). They may affect the loss of water and the wettability of surfaces. Hairs might also function as an anchor for seed dispersal by animals or wind. Some of the hairs form hooks for climbing purposes. On climbing kidney shoots, (*Phaseolus vulgaris*) hairs form hooks (figure 12*a*), and in *Cynoglossum officinale* (figure 12*b*), the hairs have lateral barbed hooks for seed dispersal (Wagner *et al.* 2004; Koch *et al.* 2009).

Velcro effect

Fruits of the burdock plant consist of hooks. Cockleburs get attached to clothes readily. In 1948, Swiss engineer George de Mestal found that their spines were tipped with tiny hooks that stick out from the seeds and provide

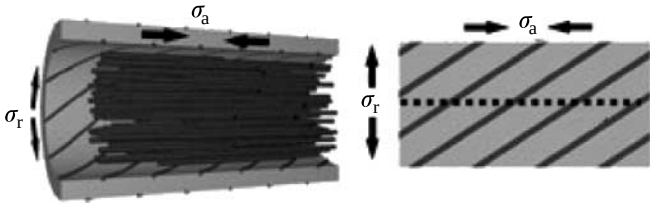

Figure 14. Schematic of a tension wood cell structure, consisting of spirally wound cellulose fibres and parallel G-layer fibres. By exposure to high humidity, swelling of the G-layer pushes against the spirally wound secondary cell wall and results in contraction of the cell along its length, resulting in high-tensile stresses leading to motion (Goswami *et al.* 2008). σ_r, circumferential hoop stress; σ_a, axial stress.

a hook-and-loop construction, which grips instantly, but can be ungripped with a light force (figure 13*a*). This led to the invention of a zip, called Velcro (1955), which works as a zipper (figure 13*b*). One side has stiff hooks as the burs and the other has loops in the fabric. The word Velcro was derived from the French words velour (velvet) and crochet (hook).

(iii) *Plant structures for motion*

Plant tissues are composite materials consisting of hierarchical structures. Some of the structures (such as wood) exhibit high stiffness, strength and resilience. Dead tissues on some plants can change shape in a controlled manner with a change in external conditions, such as temperature or humidity (Elbaum *et al.* 2008; Fratzl *et al.* 2008). The change in shape actuates movement. As an example, wheat awns are attached to the seed, which assist in the dispersion and mobility of the seed. The cellulose fibrils within a single awn are parallel on one side and randomly oriented on the other. A change in humidity causes differential swelling on either side of the awn, resulting in a reversible bending of the awn. Repeated variations in humidity from the changes in day/night temperature push the seed into the ground (Elbaum *et al.* 2008). Another example of shape change is the tension wood fibres found in the upper parts of the branches of hardwoods (figure 14; Fratzl *et al.* 2008). The tension wood fibres can generate high-tensile stresses and pull leaning stems and branches upwards. In comparison with regular fibres, tension wood cells are filled with an extra layer of cellulose and consist of parallel G-layer fibres oriented along the cell and branch axis. The outside of the tension wood consists of spirally wound cellulose. Exposure to humidity results in swelling of the parallel G-layer fibres in the radial direction pushing against the outer cell wall. The circumferential hoop stress is converted into a contraction of the cell along its length, resulting in high-tensile stresses that can actuate the movement, i.e. the change of curvature of the axis (Goswami *et al.* 2008).

To provide movement in composite mimicking plant cells, Sidorenko *et al.* (2007) developed a hydrogel matrix with embedded stiff parallel silicon needles. The isotropic swelling of the matrix is hindered by the presence of the undeformable elements, which results in anisotropic deformation. The movement can also result from the swelling of the gel.

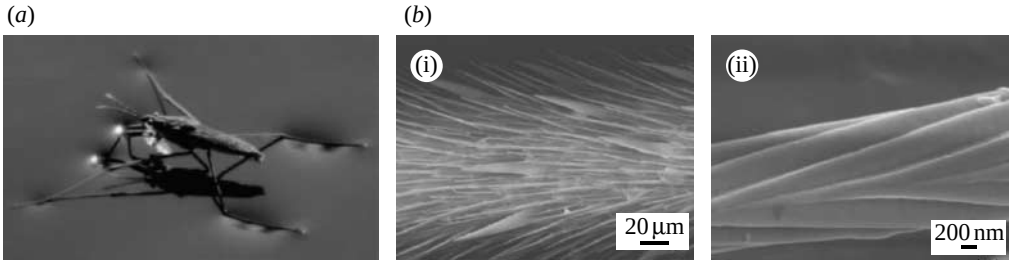

Figure 15. (*a*) Pond skater (*G. remigis*) walking on water and (*b*) SEM images of a pond skater leg showing (i) numerous oriented microscale setae and (ii) nanoscale grooved structures on a seta (Gao & Jiang 2004).

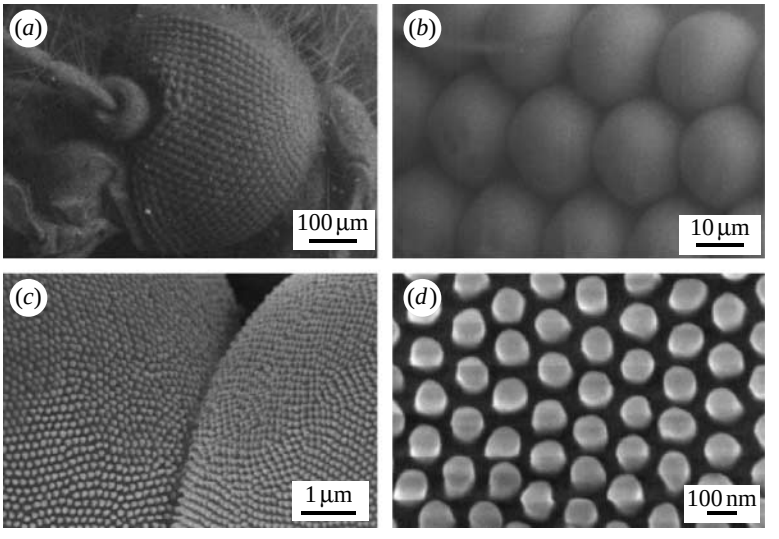

Figure 16. SEM images of (*a*) a single mosquito eye, (*b*) an HCP microhemisphere (ommatidia), (*c*) two neighbouring ommatidia and (*d*) hexagonally NCP nanonipples covering an ommatidial surface (Gao *et al.* 2007*b*).

(*c*) *Superhydrophobicity in insects*

Pond skaters (*Gerris remigis*) are insects that live on the surfaces of ponds, slow streams and quiet waters. A pond skater has the ability to stand and walk upon a water surface without getting wet (figure 15*a*). Even the impact of rain droplets with a size greater than the pond skater's size does not make it immerse into the water. Gao & Jiang (2004) showed that the special hierarchical structure of the pond skater's legs, which are covered by large numbers of oriented tiny hairs (microsetae) with fine nanogrooves and covered with cuticle wax, makes the leg surfaces superhydrophobic, is responsible for the water resistance and enables them to stand and walk quickly on the water surface. They measured the contact angle of the insect's legs with water to be approximately 167°. Scanning electron microscope (SEM) micrographs revealed numerous oriented setae on the legs (figure 15*b*). The setae are needle-shaped hairs with diameters ranging from

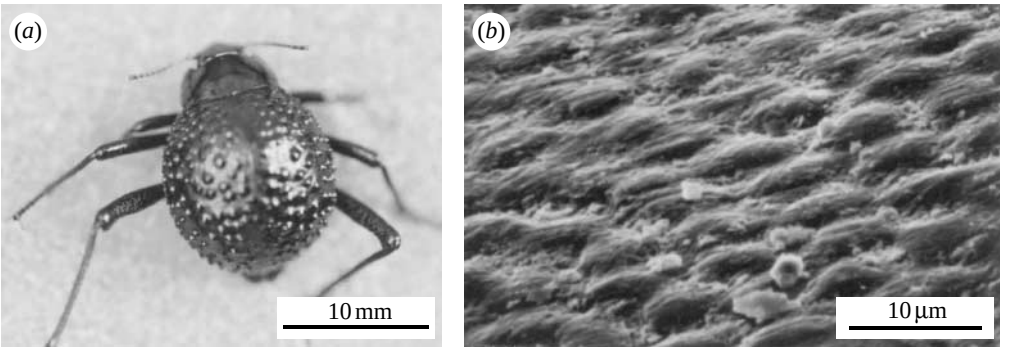

Figure 17. The water-capturing surface of the fused overwings (elytra) of the desert beetle *Stenocara* sp. (*a*) Adult female, dorsal view; peaks and valleys are evident on the surface of the elytra and (*b*) SEM image of the textured surface of the depressed areas (Parker & Lawrence 2001).

3 µm down to several hundred nanometres. Most setae are roughly 50 µm in length and arranged at an inclined angle of approximately 20° from the surface of the leg. Many elaborate nanoscale grooves were found on each microseta, and these form a unique hierarchical structure. This hierarchical micro- and nanostructuring on the leg's surface seems to be responsible for its water resistance (Nosonovsky & Bhushan 2008*a*,*b*) and the strong supporting force. Gao & Jiang (2004) reported that a leg does not pierce the water surface until a dimple of 4.4 mm depth is formed. They found that the maximal supporting force of a single leg is 1.52 mN, or approximately 15 times the total body weight of the insect. The corresponding volume of water ejected is roughly 300 times that of the leg itself.

Mosquito eyes exhibit superhydrophobic antifogging properties to provide excellent vision. An SEM micrograph of a single eye is shown in figure 16*a*. It is composed of hundreds of microscale microspheres (figure 16*b*) called ommatidia, which act as individual sensory units. These ommatidia are 26 µm in diameter and organize in a hexagonal closed packed (HCP) arrangement. The surface of each microsphere is covered with nanoscale nipples (figure 16*c*). At increasing magnification, it is observed that the nipples have an average diameter of 101 nm with a pitch of 47 nm and organize in a non-close-packed (NCP) array (figure 16*d*; Gao *et al.* 2007*b*). It is the hierarchical structure that is responsible for superhydrophobicity (Nosonovsky & Bhushan 2008*a*,*b*).

Some beetles (figure 17) in the Namib Desert in South Africa, such as the darkling beetle, collect drinking water from wind-driven morning fog by crouching with their backs raised facing the wind (figure 17). Droplets form on the top (front) fused 'wings' (elytra) and roll down the beetle's surface to its mouthparts. These large droplets form by virtue of the insect's bumpy surface, which consists of alternating hydrophobic, wax-coated and hydrophilic, non-waxy regions (Parker & Lawrence 2001). Experiments with artificial fog showed the feasibility of this mechanism, and artificial surfaces, consisting of altering hydrophobic and hydrophilic regions for biomedical applications, have been suggested (Gillmor *et al.* 2000). Other applications include water-trapping tents and building coverings. For antifogging coatings, Zhai *et al.* (2006) fabricated hydrophilic patterns on superhydrophobic surfaces with water-harvesting characteristics.

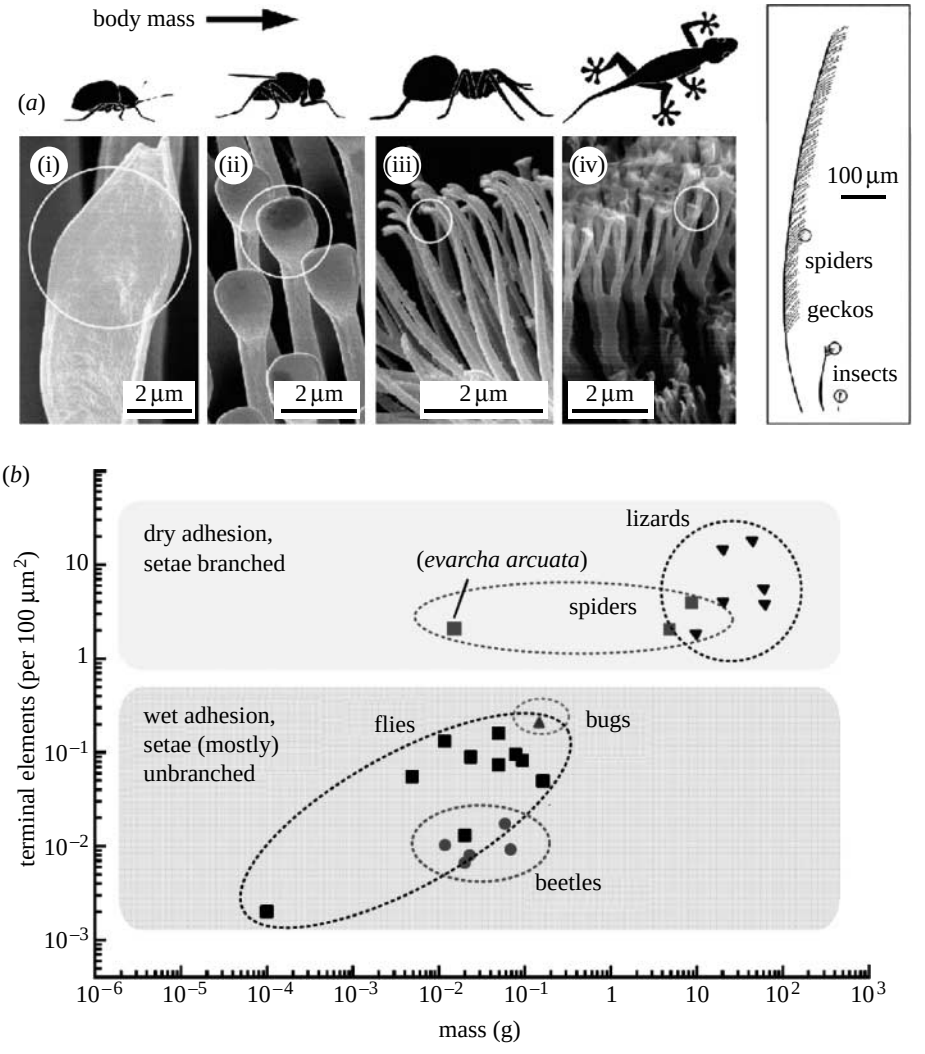

Figure 18. (*a*) Terminal elements of the hairy attachment pads of a (i) beetle, (ii) fly, (iii) spider, and (iv) gecko (Arzt *et al.* 2003) shown at different scales (left and right) and (*b*) the dependence of terminal element density on body mass (Federle 2006).

(*d*) *Adhesion in insects, spiders, lizards and frogs*

(i) *Dry adhesion*

Leg attachment pads of several animals, including many insects (e.g. beetles and flies), spiders and lizards (e.g. geckos), are capable of attaching to a variety of surfaces and are used for locomotion, even on vertical walls or across ceilings (Autumn *et al.* 2000; Gorb 2001; Bhushan 2007*b*, 2008). Biological evolution over a long period of time has led to the optimization of their leg attachment systems. This dynamic attachment ability is referred to as reversible adhesion or smart adhesion (Bhushan 2007*b*, 2008).

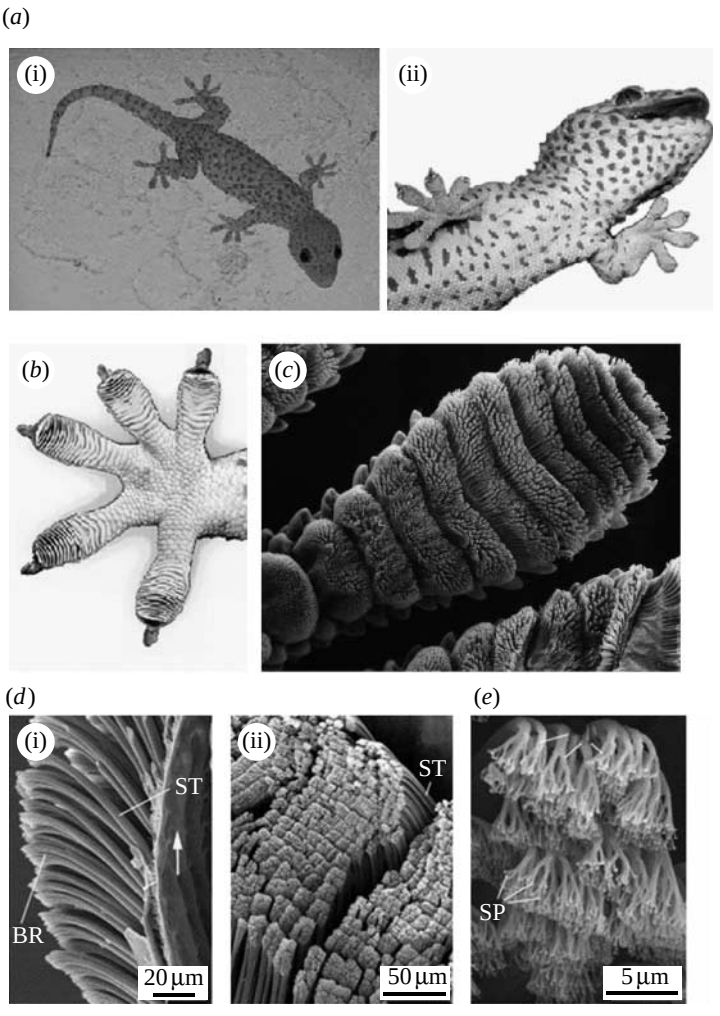

Figure 19. (*a*) Tokay gecko looking (i) top-down and (ii) bottom-up (Autumn *et al.* 2000). The hierarchical structures of a gecko foot (*b*) a gecko foot (Autumn *et al.* 2000) and (*c*) a gecko toe (Autumn 2006). Each toe contains hundreds of thousands of setae and each seta contains hundreds of spatula. SEM micrographs (at different magnifications) of (*d*) the setae (Gao *et al.* 2005) and (*e*) the spatula (Gao *et al.* 2005). ST, seta; SP, spatula; BR, branch.

Attachment systems in various creatures, such as insects, spiders and lizards, have similar structures. The microstructures used by beetles, flies, spiders and geckos can be seen in figure 18*a* (Arzt *et al.* 2003). As the size (mass) of the creature increases, the radius of the terminal attachment elements decreases (Arzt *et al.* 2003; Federle 2006). This allows a greater number of setae to be packed into an area, hence increasing the linear dimension of contact and the adhesion strength (figure 18*b*). Based on surface energy approach, it has been reported that adhesion force is proportional to a linear dimension of the contact (Bhushan 1999, 2002). Therefore, it increases with the division of contacts. The density of the terminal attachment elements, ρ_A, per m^2 strongly increases with increasing body mass, m, in g (figure 18*b*). Flies and beetles have the largest

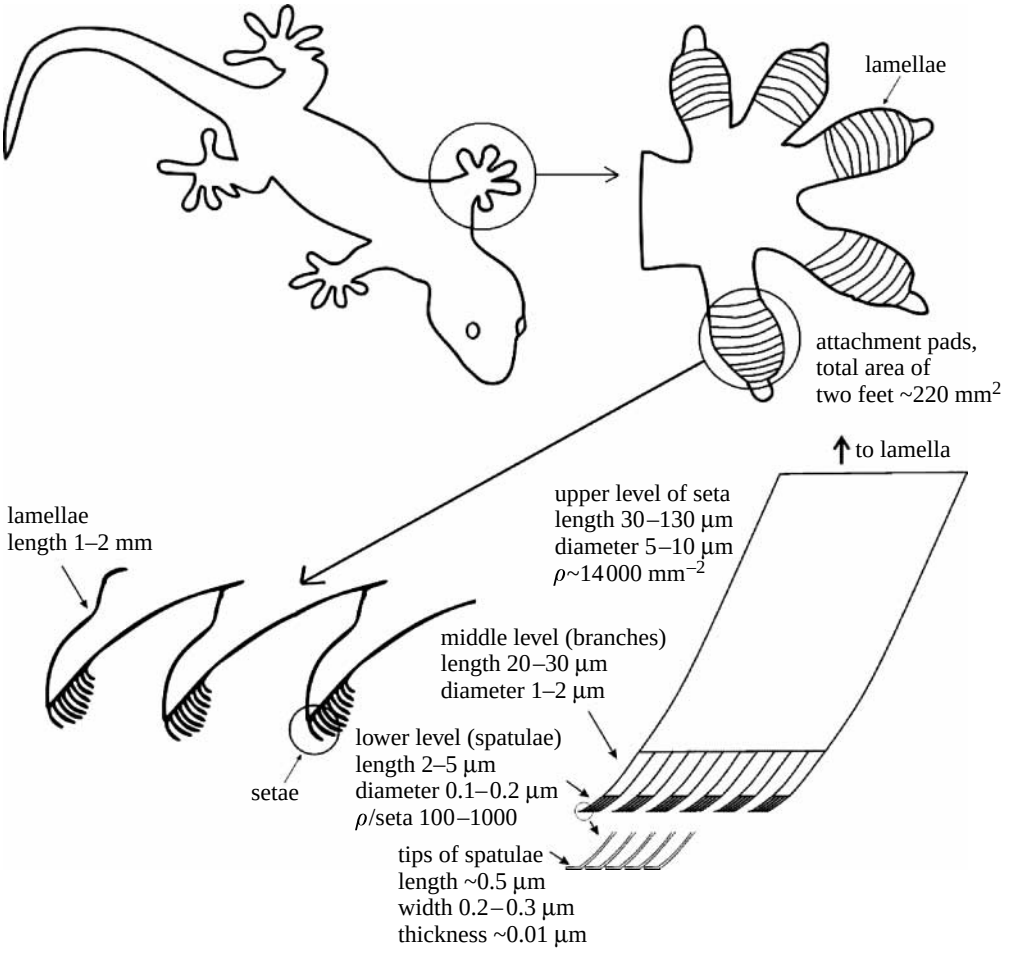

Figure 20. Schematic structure of a Tokay gecko, including the overall body, one foot, a cross-sectional view of the lamellae and an individual seta. ρ represents the number of spatula (Bhushan 2007*b*).

attachment pads and the lowest density of terminal attachment elements. Spiders have highly refined attachment elements that cover their legs. Geckos have both the highest body mass and the greatest density of terminal elements (spatula). Spiders and geckos can generate high dry adhesion, whereas beetles and flies increase adhesion by secreting liquids at the contacting interface.

A gecko is the largest animal that can produce high (dry) adhesion to support its weight with a high factor of safety. The gecko skin comprises a complex hierarchical structure of lamellae, setae, branches and spatula (Autumn *et al.* 2000; Bhushan 2007*b*). As shown in figures 19 and 20, the gecko consists of an intricate hierarchy of structures beginning with lamellae, soft ridges that are 1–2 mm in length, located on the attachment pads (toes) that compress easily so that contact can be made with rough bumpy surfaces. Tiny curved hairs, known as setae, extend from the lamellae with a density of approximately 14 000 mm^{-2}. These setae are typically 30–130 μm in length and 5–10 μm in diameter and are primarily composed of β-keratin with some α-keratin components. At the end of each seta, 100–1000 spatulae, with a diameter of 0.1–0.2 μm, branch out and

form the points of contact with the surface. The tips of the spatula are approximately 0.2–0.3 μm in width, 0.5 μm in length and 0.01 μm in thickness, and get their name from their resemblance to a spatula.

The attachment pads on two feet of the Tokay gecko have an area of approximately 220 mm^2. Approximately 3×10^6 setae on their toes can produce a clinging ability of approximately 20 N (vertical force required to pull a lizard down a nearly vertical (85°) surface) and allow them to climb vertical surfaces at speeds of over 1 $m\,s^{-1}$, with the capability to attach or detach their toes in milliseconds. It should be noted that a three-level hierarchical structure allows adaptability to surfaces with different magnitudes of roughness. The gecko uses a peeling action to unstick itself (Bhushan 2007*b*, 2008).

Replication of the structure of gecko feet would enable the development of a superadhesive polymer tape capable of clean, dry adhesion, which is reversible (e.g. Geim *et al.* 2003; Bhushan 2007*b*, 2008; Bhushan & Sayer 2007; Gorb *et al.* 2007). (It should be noted that common man-made adhesives, such as tape or glue, involve the use of wet adhesives that permanently attach two surfaces.) The reusable gecko-inspired adhesives have the potential for use in everyday objects, such as tapes, fasteners and toys, and in high technology, such as microelectronic and space applications. Replication of the dynamic climbing and peeling ability of geckos could find use in the treads of wall-climbing robots (Cutkosky & Kim in press).

(ii) *Wet adhesion*

Some amphibians, such as tree and torrent frogs and arboreal salamanders, are able to attach to and move over wet or even flooded environments without falling (Federle *et al.* 2006). Tree frog toe attachment pads consist of a hexagonal array of flat-topped epidermal cells of approximately 10 μm in size separated by approximately 1 μm wide mucus-filled channels; the flattened surface of each cell consists of a submicrometre array of nanopillars or pegs of approximately 100–400 nm diameter (figure 21). The toe pads are made of an extremely soft, inhomogeneous material; the epithelium itself has an effective elastic modulus of approximately 15 MPa, equivalent to silicone rubber (Scholz *et al.* 2009). The pads are permanently wetted by mucus secreted from glands that open into the channels between epidermal cells. They attach to mating surfaces by wet adhesion (Federle *et al.* 2006). They are capable of climbing on wet rocks even when water is flowing over the surface (Barnes *et al.* 2002).

The pad structure is believed to produce high adhesion and friction by conforming to the mating rough surface at different length scales and by maintaining a very thin fluid film at the interface, responsible for animal locomotion and manoeuvrability. Adhesion is believed to occur primarily by a meniscus contribution, resulting from menisci formed around the edges of the pads (Federle *et al.* 2006). The presence of static friction suggests that the fluid film is very thin in order to have some dry contact between the tips of the nanopillars and the mating surface. The dry contacts between the pad and the mating surfaces are produced by squeezing out the fluid film from the interface. Hierarchical structure and material properties facilitate the squeezing and avoid formation of trapped liquid islands during draining, which would favour sliding (Federle *et al.* 2006). During walking, the squeezing is expected to

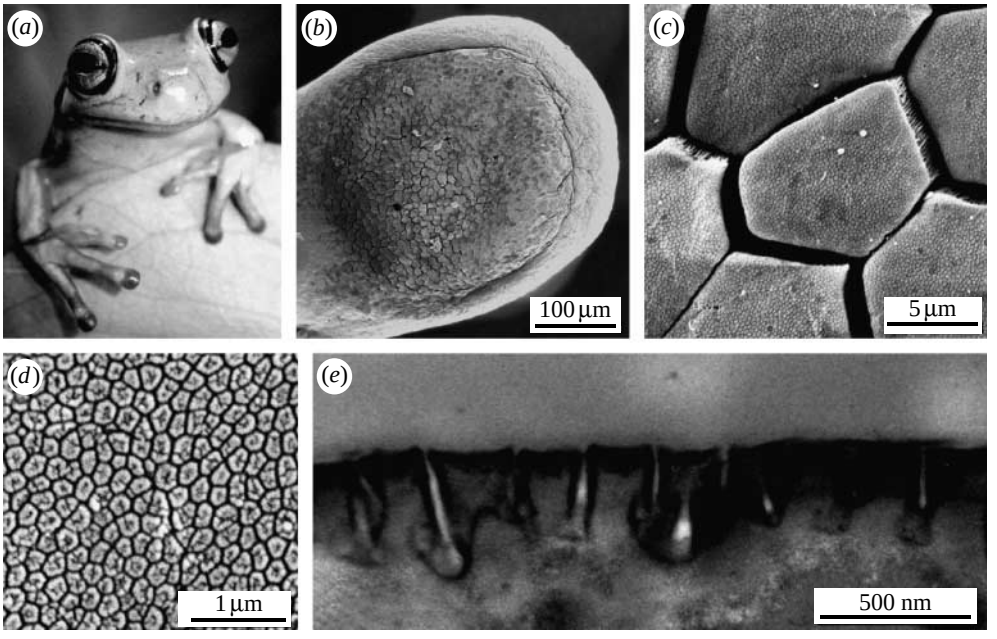

Figure 21. Morphology of tree frog toe pads. (*a*) White tree frog (*Litoria caerulea*). SEM images of (*b*) toe pad, (*c*) epidermis with hexagonal epithelial cells, (*d*) high-magnification image of the surface of a single hexagonal cell showing peg-like projections, and (*e*) transmission electron microscope image of cross section through cell surface (Federle *et al.* 2006).

occur rapidly. Torrent frogs can resist sliding, even on flooded surfaces. The surface of their toe pads is similar to that of tree frogs with some changes in the structure to handle the large flow of water (Ohler 1995).

The structure of the toe pads of tree and torrent frogs can be used in the development of structures with reversible adhesion under wet or flooded conditions. The treads of tyres used in transport vehicles are inspired by the patterns on the toe pads of tree frogs. On wet roads, water/snow flows out through channels present between the treads. This provides an intimate contact between the tyre treads and the road leading to high adhesion, which is responsible for good grip while driving on the wet road.

(*e*) *Aquatic animals*

(i) *Low hydrodynamic drag*

Many aquatic animals can move in water at high speeds, with a low energy input. Drag is a major hindrance to movement. Most shark species move through water with high efficiency and maintain buoyancy. Through its ingenious design, their skin turns out to be an essential aid in this behaviour by reducing drag by 5–10 per cent and autocleaning ectoparasites from their surface (Bechert *et al.* 1997, 2000). The very small individual tooth-like scales of shark skin, called dermal denticles (little skin teeth), are ribbed with longitudinal grooves (aligned parallel to the local flow direction of the water), which result in water moving very efficiently over their surface. An example of scale structure on

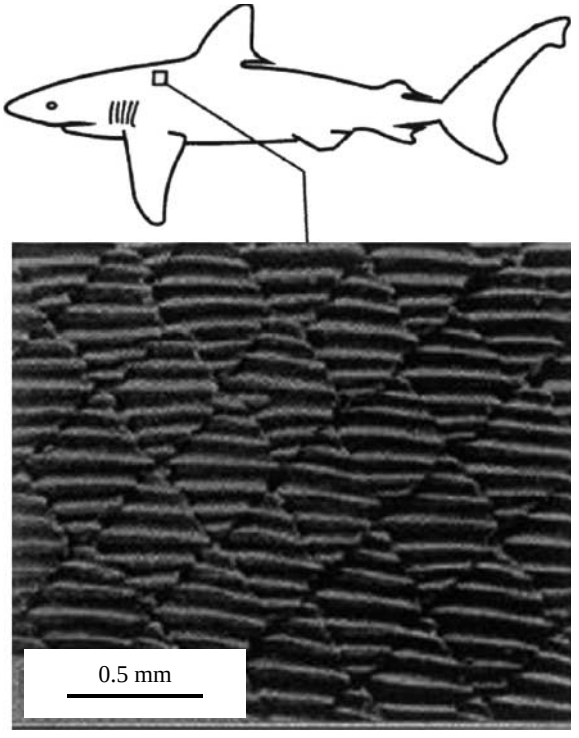

Figure 22. Scale structure on a Galapagos shark (*C. galapagensis*; Reif 1985).

the right front of a Galapagos shark (*Carcharhinus galapagensis*) is shown in figure 22. The detailed structure varies from one location to another for a given shark. The scales are present over most of the shark's body. These are V-shaped, approximately 200–500 μm in height, and regularly spaced (100–300 μm).

Owing to the relatively high Reynolds number of a swimming shark, turbulent flow occurs. The skin drag (wall shear stress) is not generally affected by surface roughness. Longitudinal scales on the surface result in lower wall shear stresses than that on a smooth surface and control boundary-layer separation. The longitudinal scales result in water moving more efficiently over their surface than it would were shark scales completely featureless. Over smooth surfaces, fast-moving water begins to break up into turbulent vortices, or eddies, in part because the water flowing at the surface of an object moves slower than water flowing further away from the object with so-called low boundary slip. This difference in water speed causes the faster water to get 'tripped up' by the adjacent layer of slower water flowing around an object, just as upstream swirls form along riverbanks. The grooves in a shark's scales simultaneously reduce eddy formation in a surprising number of ways: (i) the grooves reinforce the direction of flow by channelling it, (ii) they speed up the slower water at the shark's surface (as the same volume of water going through a narrower channel increases in speed), reducing the difference in speed of this surface flow and the water just beyond the shark's surface, (iii) conversely, they pull faster water towards the shark's surface so that it

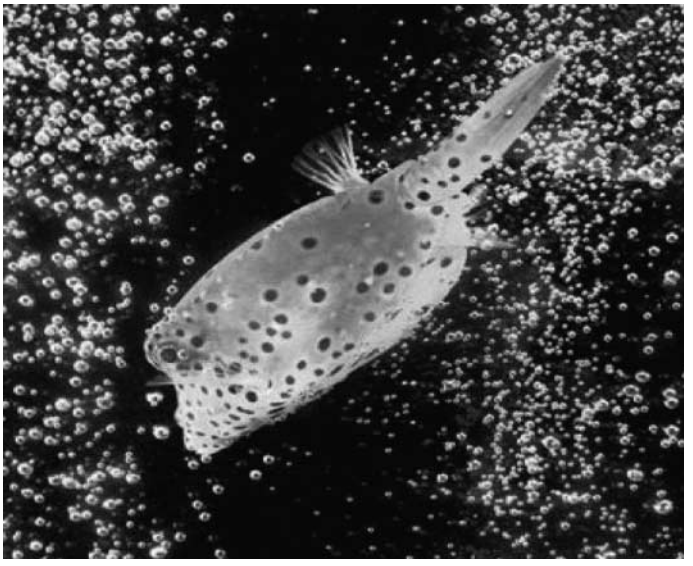

Figure 23. The image of a boxfish (*O. meleagris*).

mixes with the slower water, reducing this speed differential, and finally, (iv) they divide up the sheet of water flowing over the shark's surface so that any turbulence created results in smaller, rather than larger, vortices (www.biomimicryinstitute.org).

It is also reported that longitudinal scales influence the fluid flow in the transverse direction by limiting the degree of momentum transfer. It is the difference in the protrusion height in the longitudinal and transverse directions that governs how much the scales impede the transverse flow. Bechert *et al.* (1997) reported that, based on their experimental data, thin, vertical scales result in low transverse flow and low drag. They also reported that the ratio of scale height to tip-to-tip spacing of 0.5 is the optimum value for low drag.

In addition to reduction of drag, the shark skin surface prevents marine organisms from being able to adhere to ('foul') it. It is not because of the lotus effect, but the shark skin is hydrophilic and wets with water. There are three factors that appear to keep the surface clean: (i) the accelerated water flow at a shark's surface reduces the contact time of fouling organisms, (ii) the roughened nanotexture of shark skin reduces the available surface area for adhering organisms, and (iii) the dermal scales themselves perpetually realign or flex in response to changes in internal and external pressure as the shark moves through water, creating a 'moving target' for fouling organisms (www.biomimicryinstitute.org).

Speedo created the whole body swimsuit called Fastskin bodysuit (TYR Trace Rise) in 2006 for elite swimming. The suit is made of polyurethane woven fabric with a texture based on shark scales. In the 2008 Summer Olympics, two-thirds of the swimmers wore Speedo swim suits, and a large number of world records were broken. Boat, ship and aircraft manufacturers are trying to mimic shark skin to reduce friction drag and minimize the attachment of organisms on their bodies. One can create riblets on the surface by painting or attaching a film (3M). Skin friction contributes to about half of the total drag in an aircraft. Transparent sheets with a

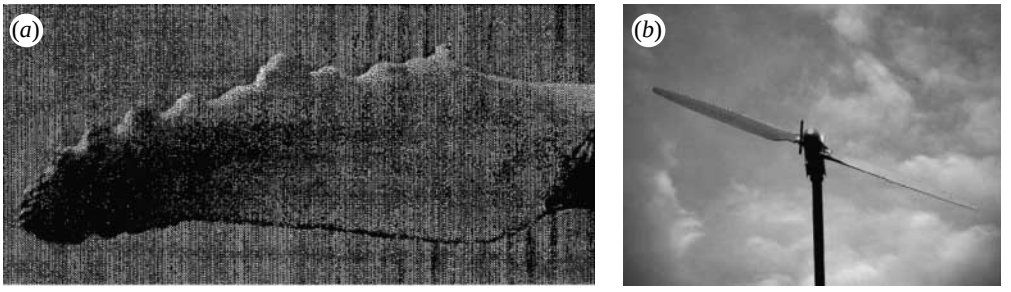

Figure 24. (*a*) Scalloped edges of a humpback whale used to make tight turns and (*b*) design of turbine blades with tubercles to reduce drag in wind turbines (Fish & Battle 1995; Fish 2006).

ribbed structure in the longitudinal direction have been used on the commercial Airbus 340 aircraft. It is expected that riblet film on the body of the aircraft can reduce drag of the order of 10 per cent (Fish 2006).

Mucus on the skin of aquatic animals, including sharks, acts as an osmotic barrier against the salinity of sea water and protects the creature from parasites and infections (Bechert *et al.* 2000). The mucus also operates as a drag-reducing agent on some fast predatory fishes, which allows the fishes to attack more easily (Hoyt 1975). The artificial derivatives of fish mucus, i.e. polymer additives for liquids, are used in drag reduction technology, for example, to propel crude oil in the Alaska pipeline (Motier & Carrier 1989).

The compliant skin of dolphins allows the high speed of dolphins. The compliant skin, interacting with the water flowing over the body's surface, stabilizes the flow and delays transition to turbulence. The delay in the onset of turbulence is believed to reduce skin friction and drag. It has been reported that dolphin skin would also work under fully turbulent flow conditions; however, the drag reduction is expected to be small, a few per cent (Bechert *et al.* 2000). Dolphins possess an optimum shape for drag reduction of submerged bodies. Submarines use the shape of dolphins.

The boxfish (*Ostracion meleagris*) has a streamlined form with squared-off contours, shown in figure 23 (Mueller 2008). The body provides a low drag, and the fish can swim up to six body lengths per second. Its shape inspired Mercedes Benz's bionic concept car with a low aerodynamic drag, providing high fuel economy.

Finally, in contrast to seabirds or boat surfaces, fishes are not endangered by pollution from oil during an oil spill because their surfaces are superoleophobic. These surfaces should be superior to the traditional approach employing surfactant solutions to aid in the removal of oil from the surfaces, as these surfaces would be ecologically friendly.

(ii) *Energy production*

Humpback whales have scalloped edges with a unique series of bumps called tubercles on their flippers (figure 24). Fish & Battle (1995) reported that the tubercles enable these huge whales to make very tight turns in manoeuvring to secure their food. Inspired by this, Fish (2006) designed wind turbine blades with tubercles approximately 0.7 m tall (figure 24). Based on wind tunnel tests, his group reported that blades with tubercles, as compared with those without tubercles, exhibited an increase in the angle of attack (the angle that a blade makes into the

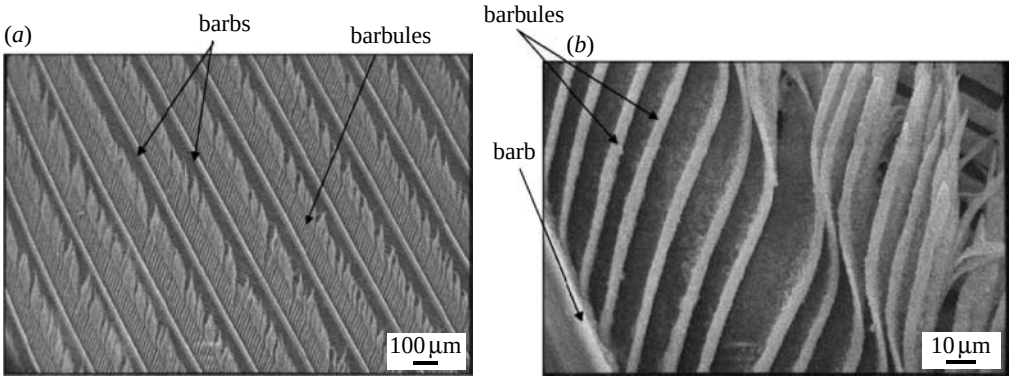

Figure 25. (*a*,*b*) SEM images of pigeon feather structure at two magnifications (Bormashenko *et al.* 2007).

Figure 26. The wings of a bird in landing approach.

incident wind) from 11 to 17° prior to stalling. These blades with tubercles for wind turbines can be used to improve performance at low wind speeds by increasing the angle of attack without stalling. Fish (2006) reported that tubercles enable the flipper to decrease drag, which allows the humpback whale to use less energy to turn.

(*f*) *Birds*

Bird feathers perform multiple functions—make the body water repellant, create wings and tails for aerodynamic lift during flying, provide coloration for appearance as well as camouflage and provide an insulating layer to keep the body warm.

(i) *Hydrophobicity*

Many bird feathers exhibit hydrophobicity (an apparent contact angle of 100–140°). Bormashenko *et al.* (2007) studied Feral Rock pigeon feathers. An SEM image of the pigeon feather (pennae) is shown in figure 25. The morphology consists of a network formed by barbs and barbules made of keratin. It is the morphology that plays an important role in hydrophobicity.

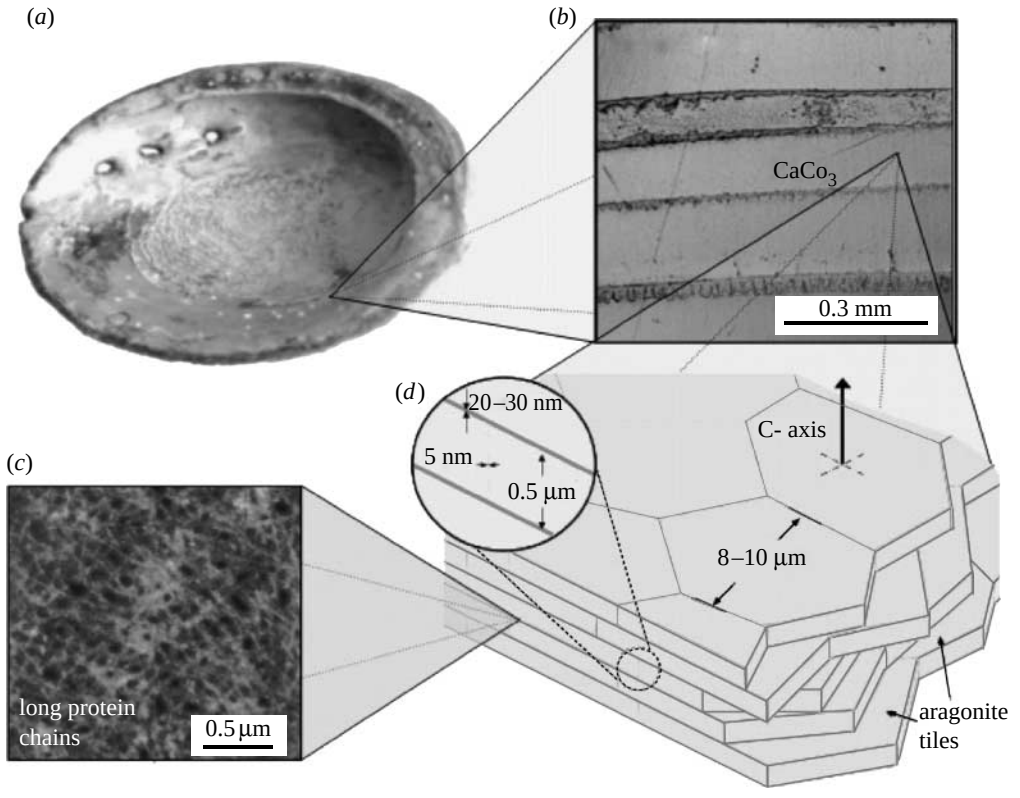

Figure 27. Hierarchy of the abalone structure. (*a*) Entire shell, (*b*) mesostructure with mesolayers, (*c*) nanostructure showing organic interlayer comprising 5 wt% of overall shell, and (*d*) microstructure with aragonite tiles (Meyers *et al.* 2006).

(ii) *Aerodynamics*

Birds consist of several consecutive rows of covering feathers on their wings, which are flexible (figure 26). These movable flaps develop the lift. When a bird lands, a few feathers are deployed in front of the leading edges of the wings, which help to reduce the drag on the wings. Self-activated movable flaps (artificial bird feathers) have been shown to provide an increase in lift in flight experiments (Bechert *et al.* 2000). Birds serve as the inspiration for aircraft and early developments of wing design (Jakab 1990). However, aircraft do not flap their wings like birds to simultaneously produce lift and thrust. This is impractical in aircraft due to limitations of scaling phenomena and high speeds.

The favourable aerodynamics of the beak of a kingfisher was used to model the nose cone of the Japanese Shinkansen bullet train.

(iii) *Hues*

Various birds (e.g. peacocks) and butterflies create brilliant hues by refracting light through millions of repeating structures that bend light to make certain colours. They do not use pigments. For example, the only pigment in peacock feathers is brown. These studies are being used to develop brighter screens for cellular phones.

(*g*) *Seashells*

Seashells are biominerals that are natural nanocomposites with a laminated structure. They exhibit superior mechanical properties to their constituents (Lowenstam & Weiner 1989; Sarikaya & Aksay 1995; Mann 2001; Meyers *et al.* 2006, 2008). This is because biological organisms produce composites that contain both inorganic and organic components in complex structures. The mineral is embedded in a complex assemblage of organic macromolecules that are hierarchically organized. The mineral component provides the strength, and the organic components provide the ductility. Seashells are composed of a large fraction of inorganic minerals (typically calcium carbonate, calcium phosphate and amorphous silica with a concentration of the order of 95%) and a small fraction of organic biopolymers (typically keratin, collagen and chitin in the range of 1–5%).

A large variety of shells are found in nature (Meyers *et al.* 2006, 2008). The one most studied is the abalone shell (Haliotis). Abalone shells derive their extraordinary mechanical properties (compared to monolithic $CaCO_3$) from a hierarchically organized structure, starting at the nanolevel with a 20–30 nm thick organic layer, proceeding with single crystals of the aragonite polymorph of $CaCO_3$, consisting of 0.5–10 μm thick bricks (microstructure), and finishing with 0.3 mm thick layers (macrostructure) (figure 27) (Meyers *et al.* 2006). Between the layers of shells is a 20–30 nm thick organic protein substance, such as chitin, lustrin and silk-like proteins. This mixture of brittle platelets and thin layers of elastic biopolymers inhibit transverse crack propagation and make the material strong and resilient. The multiple-length sizes significantly increase its toughness, making it equivalent to silicon. Mechanisms for the growth and self-assembly of aragonitic calcium carbonate found in the shell of the abalone have been studied by Lin & Meyers (2005).

The shells of abalones have a low and open spiral structure. The thick inner layer of the shell is composed of nacre, also known as mother of pearl. Nacre is strong and iridescent with changeable colours, and is used for decorative purposes. It is called mother of pearl because it is literally the mother or creator of the pearl. The deformation mechanisms and mechanics of nacre have been investigated by Wang *et al.* (2001) and Barthelat *et al.* (2007). Mechanical properties of nacre have been measured (Jackson *et al.* 1988; Sarikaya *et al.* 1990; Li *et al.* 2004). Jackson *et al.* (1988) reported an elastic modulus of approximately 70 GPa (dry) and 60 GPa (wet) from the shell of a bivalve mollusc, *Pintada umbricata*, and a tensile strength of approximately 170 MPa (dry) and 130 MPa (wet). Sarikaya *et al.* (1990) reported fracture toughness of approximately 8 MPa $m^{1/2}$, measured using four-point bending tests, and a fracture strength of approximately 185 MPa in three-point bending tests, which are superior to that of many engineering ceramics. Fracture toughness is reported to increase in wet conditions. The moisture has a significant plasticizing effect on proteinaceous layers and leads to an increase in toughness.

There have been attempts to fabricate artificial nacre (e.g. Tang *et al.* 2003; Munch *et al.* 2008; Luz & Mano 2009).

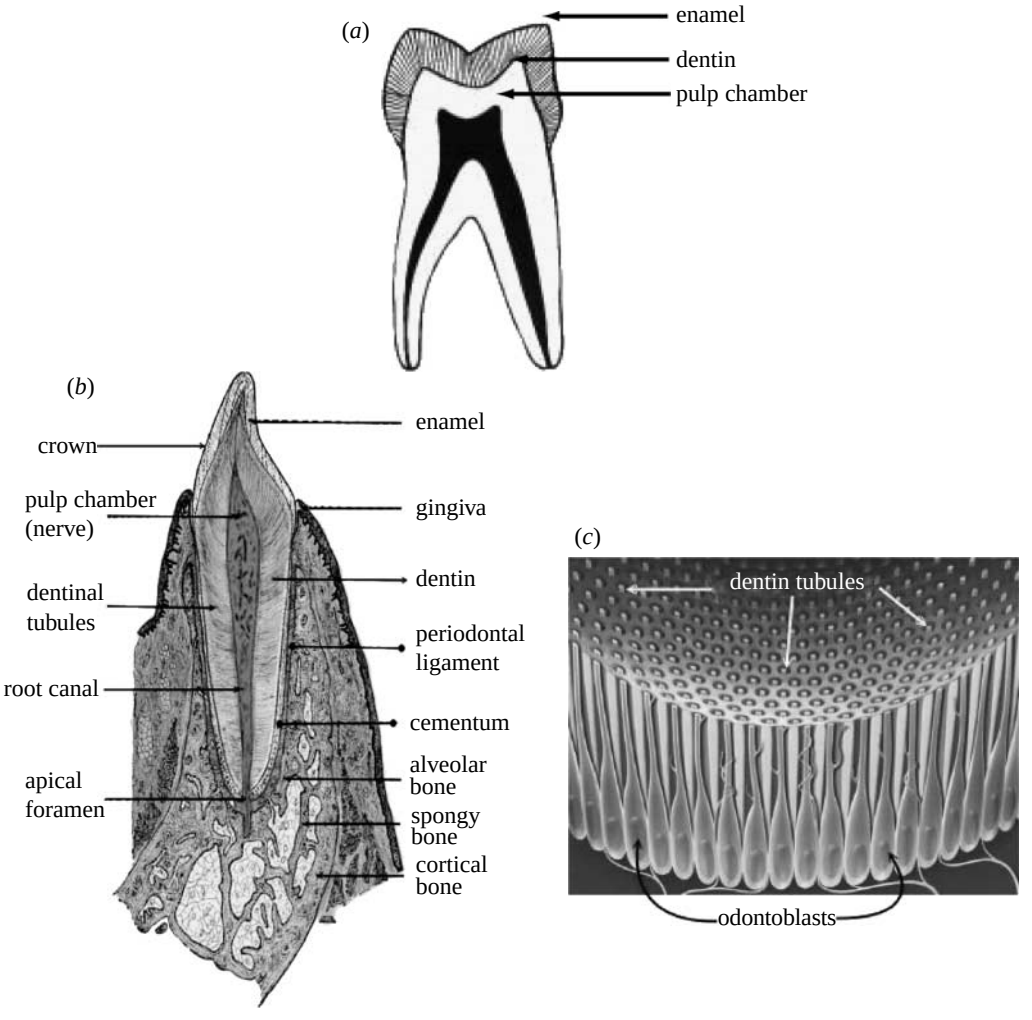

Figure 28. (*a*) Overall schematic of an individual human tooth, (*b*) detailed anatomy of the tooth showing its hierarchical structure, and (*c*) structure of dentin comprising thousands of dentinal tubules (www.doctorspiller.com).

(*h*) *Bones and teeth*

Bones are hard biological tissues (Lowenstam & Weiner 1989; Sarikaya & Aksay 1995; Mann 2001; Alexander & Diskin 2004). These exhibit excellent mechanical strength, primarily because of their hierarchical structure. The toughness of the bone originates from its ability to dissipate deformation energy at different levels of its structure (Fratzl 2008), as well as sacrificial bonds in organic layers around individual collage fibrils (Fantner *et al.* 2005).

An individual tooth consists of two major parts: the crown and the root (Linde & Goldberg 1993; figure 28*a*). The tooth itself consists of a multilayered structure with the crown as the outer layer, the dentin layer as an intermediate layer and the pulp chamber in the core part (Schroeder 1991; figure 28*b*). The outer layer of the crown is made of enamel, and the root part is covered by

Figure 29. The spiderweb made of silk material (Bar-Cohen 2006).

cementum. The enamel is the mineralized tissue. It is acellular and consists of approximately 95 wt% inorganic hydroxyapatite crystallites, approximately 4 wt% water and approximately 1 wt% proteins. The dentin, which forms the bulk of the tooth, is approximately 70 wt% mineralized with hydroxyapatite crystals and also consists of approximately 20 wt% organic components (proteins, collagens and lipids) and approximately 10 wt% water. The structure of dentin comprises densely packed tubules, approximately 1–3 μm in diameter and a density of approximately 15 000 tubules mm^{-2} (figure 28*c*). They originate from the inner part of the nerve space and travel perpendicular from the point of origin to the surface to the tooth, terminating at the understructure of the enamel. The tubules contain tiny projections of cells called odontoblasts. The composition and structure of the dentin provide elasticity and mechanical strength to the teeth. Enamel, which covers the crown, is very hard and quite resistant to mechanical and chemical attack. It protects the tooth from the oral environment. In general, it is vulnerable to acid attack from excess sugar and abrasion from hard objects and cutting/chewing. The teeth are worn down continuously, but in such a way that they remain sharp and functional.

Animal jaws have teeth that are used for cutting and crushing hard objects (food). The teeth should be self-sharpening and durable. Sea urchins have teeth that can cut extremely hard objects and are durable. These teeth consist of numerous magnesium-bearing calcite plates, with a small amount of organic material. They consist of three hierarchical levels—the lantern on the centimetre scale, tooth architecture on the millimetre scale and tooth microstructure on the micrometre scale (Wang *et al.* 1997). The composition and hierarchical structure provide a combination of high toughness and elastic modulus and are responsible for extreme durability.

The understanding of composition and structure of various teeth is being used to develop dental implants and wear-resistant and self-sharpening structures, including self-sharpening knives.

(*i*) *Spiderweb*

Spiders produce a variety of proteins, among which are major ampullate silks (MAS). MAS fibres are used by spiders as a scaffold upon which they attach other silk fibres during the formation of the web. The spider generates the silk fibre and, at the same time, is hanging on it. It has a sufficient supply of raw material for its silk to span great distances (Jin & Kaplan 2003; Bar-Cohen 2006). Spiderweb is a structure built of a one-dimensional fibre (figure 29). The fibre is very strong and continuous and is insoluble in water. The web can hold a significant amount of water droplets, and it is resistant to rain, wind and sunlight (Sarikaya & Aksay 1995; Bar-Cohen 2006). Spider silk is three times stronger than steel, having a tensile strength of approximately 1.2 GPa (Vogel 2003). Some spider silks have high stiffness with a tensile modulus of approximately 10 GPa, while others are elastomeric with a modulus of approximately 1 GPa and an extension to rupture of 200 per cent. The combination of strength and extensibility is primarily derived from the domains of crystalline β-sheets and flexible helices within the polypeptide chain, imparting a toughness that is greater than bone, Kevlar and high strength steel. The web is designed to catch insects (food for the spider) that cross the net and get stuck to its stickiness and complex structure.

While mechanical properties of the web fibre are remarkable, it is also quite interesting how a spider creates a two-dimensional web out of its silk fibre. Krink & Vollrath (1997) analysed spiderweb-building behaviour using a computer model that constructed artificial webs with a rule-based simulation. They found that web characteristics, such as the spiral distances, eccentricities and vertical hub location, were accurately simulated with the model. They later proposed a 'virtual spider robot' that builds virtual webs, which perfectly mimic the visual architecture of real webs of the garden cross spider *Araneus diadematus*. They suggested that the garden spider uses web-building decision rules that are strictly local and based on the interactions with previously placed threads to generate global architecture. This may be interesting for the modelling of biological self-assembly of complex material from the local rules to the overall structure that is adaptive to the external conditions.

Researchers have used the synthesis of structural proteins to produce polymers for fibres that may become commercially useful in the future (Gosline *et al.* 1995; Reed *et al.* 2009). Dzenis (2004) suggested an electrospinning technique to produce 2 μm diameter continuous fibres from polymer solutions that are somewhat similar to the spider silk fibres.

(*j*) *Moth-eye effect and structural coloration*

Optical reflection and antireflection is achieved in nature by using nanoscale architecture (Parker in press). The eyes of moths are antireflective to visible light. The so-called moth-eye effect was discovered in the 1960s as a result of the study of insect eyes. For nocturnal insects, it is important not to reflect the light, since the reflection makes the insect vulnerable to predators. The eyes of moths

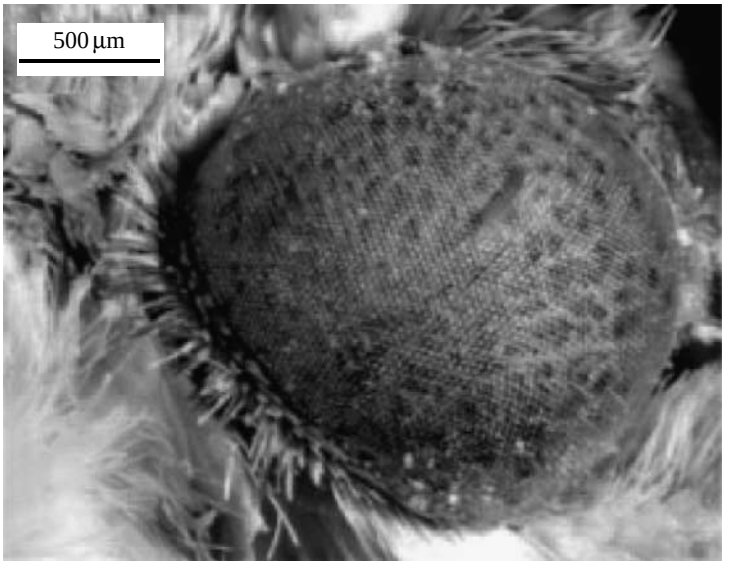

Figure 30. SEM image of a moth's eye (Genzer & Efimenko 2006).

consist of hundreds of hexagonally organized nanoscopic pillars, each approximately 200 nm in diameter and height, which result in a very low reflectance for visible light (figure 30; Genzer & Efimenko 2006; Mueller 2008). These nanostructures' optical surfaces make the eye surface nearly antireflective in any direction.

Light reflection is avoided by a continuously increasing refractive index of the optical medium. The little protuberances upon the cornea surface increase the refractive index. These protuberances are very small microtrichia (approx. 200 nm in diameter). For an increase in transmission and reduced reflection, a continuous matching of the refraction index at the boundary of the adjacent materials (cornea and air) is required. If the periodicity of the surface pattern is smaller than the light wavelength, the light is not reflected (Gorb 2006). If this condition is satisfied, it may be assumed that, at any depth, the effective refraction index is the mean of that of air and the bulk material, weighted in proportion to the amount of material present at that depth (Nosonovsky & Bhushan 2008*a*). For a moth-eye surface with the height of the protuberances of h and the spacing of d, it is expected that the reflectance is very low for wavelengths less than approximately 2.5 hours and greater than d at normal incidence, and for wavelengths greater than $2d$ for oblique incidence. For protuberances with 220 nm depth and the same spacing (typical values for the moth eye), a very low reflectance is expected for the wavelengths between 440 and 550 nm (Wilson & Hutley 1982).

This moth-eye effect should not be confused with the reduction of the specular reflectance by roughening of a surface. Roughness merely redistributes the reflected light as diffuse scattering. In the case of the moth eye, there is no increase in diffuse scattering, the transmitted wavefront is not degraded, and the reduction in reflection gives rise to a corresponding increase in transmission (Wilson & Hutley 1982).

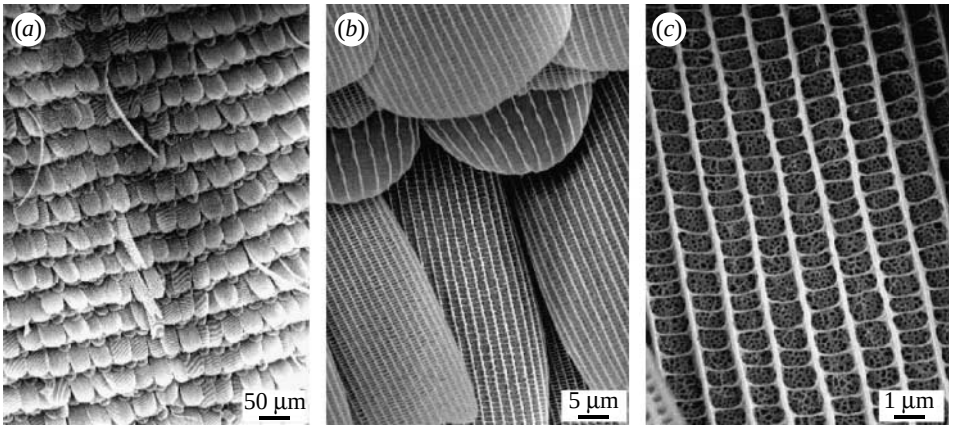

Figure 31. (*a–c*) Images of *Polyommatus icarus* (common blue) butterfly wings at different magnifications, showing that they are composed of thousands of scales with complex hierarchical structures (courtesy of W. Barthlott).

Attempts are being made to incorporate microscopic corrugations in solar panels to reduce light reflection. Attempts are also being made to produce a glare-free computer screen by creating facets on a photosensitive lacquer using lasers. Some 25×10^3 dots of texture mm^{-2} can essentially eliminate the glare on the screen (Mueller 2008). Hadobás *et al.* (2000) prepared patterned silicon surfaces with 300 nm periodicity and depth up to 190 nm. They found a significant reduction in reflectivity, partially due to the moth-eye effect. Gao *et al.* (2007*a*) used epoxy and resin to replicate the antireflective surface of a cicada's eye. It is also possible to create transparent surfaces using the moth-eye effect (Clapham & Hutley 1973).

In addition to nanostructures that lead to non-reflective surfaces, many insects, such as butterflies, use structural coloration due to the presence of scales (figure 31). The wing scales have hierarchical structure at various length scales (Gorb 2006; Kertezs *et al.* 2006). Whereas red and yellow wing colours are provided by coloured pigments, blue and green shades are provided from light scattered off the hierarchical structure on the wing. Some insects use a mechanism called iridescence, using a complex multilayer structure for optical interference. Such structures can produce complicated optical effects, including strong polarization, colour mixing and reflection angle broadening (Gorb 2006). Textile fabric, paints and cosmetics have been developed based on the surface of butterflies. It has been suggested to use this effect for the displays of various devices, such as cell phones. Unlike conventional displays that require an internal source of light and become bleak in bright light (e.g. in sunlight), the displays using biomimetic technology would work from a reflected light, would be seen well in the sunlight and consume little energy.

(*k*) *Fur and skin of polar bear*

The polar bear, one of the biggest predators on the Earth, has to survive in arctic cold, up to -50°C. A fat layer up to 100 mm thick helps protect these huge animals from cold. Owing to its black skin and white fur (figure 32*a*), the polar

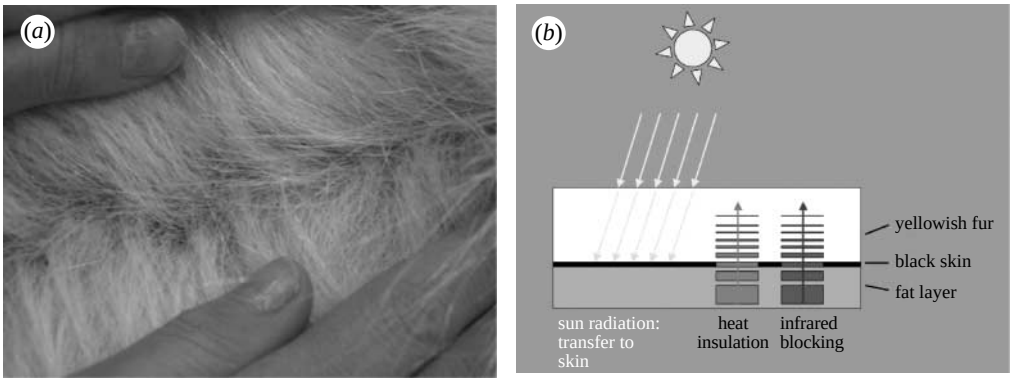

Figure 32. (*a*) Image of yellowish white fur and black skin of polar bear and (*b*) schematic of solar thermal function of polar bear fur (Stegmaier *et al.* in press).

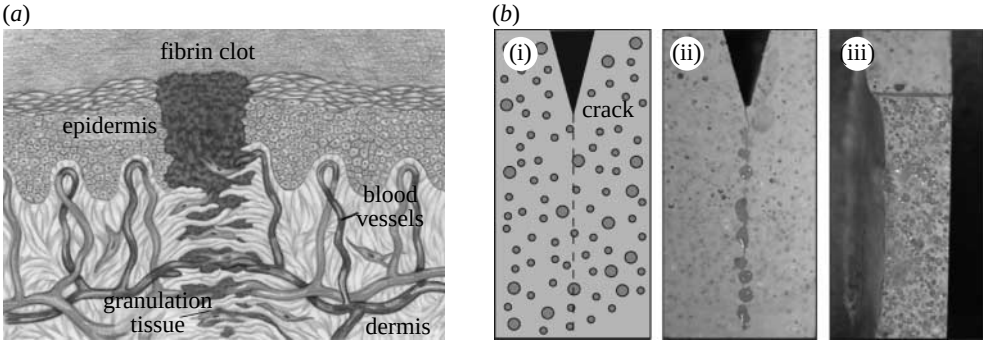

Figure 33. (*a*) Schematic of an intermediate stage of biological wound healing in skin. Tissue damage triggers bleeding, which is followed by the formation of a fibrin clot. Fibroblast cells migrate to the wound site, enabling the creation of granulation tissue to fill the wound (Singer & Clark 1999). (*b*) Demonstration of bioinspired damage-triggered release of a microencapsulated healing agent in a polymer specimen: (i) schematic of compartmentalized healing agent stored in a matrix, (ii) release of dyed healing agent into the crack plane, which leads to a synthetic slotting (polymerization) process to bond the crack faces, and (iii) one-half of the fracture surface revealing ruptured capsules (Youngblood & Sottos 2008).

bear can capture incident sunlight. The yellowish white hollow hairs reflect the sunlight along their length until it is transferred into heat in the black skin (Stegmaier *et al.* in press). Hollow hairs in the fur, together with fat skin, provide high thermal insulation (figure 32*b*). Milwich *et al.* (2006) and Stegmaier *et al.* (in press) have developed artificial furs and textiles.

(*l*) *Self-healing of biological systems*

There are several biological mechanisms of self-repair. At the molecular level, there are dynamically breaking and repairing 'sacrificial' bonds, which allow for material to deform in a quasi-plastic manner without fracture. In bones, there is a cyclic replacement of material by specialized cells, which allows for a bone to adapt to changing conditions and to repair damage. Many fractured or critically

damaged living tissues can heal themselves by the formation of an intermediate tissue (based on the response to inflammation) followed by the scar tissue (Fratzl & Weinkamer 2007).

A remarkable property of biological tissues is their ability of self-healing. In biological systems, chemical signals released at the site of fracture initiate a systemic response that transports repair agents to the site of an injury and promotes healing. The biological processes control tissue response to injury and repair involves inflammation, wound closure and matrix remodelling (figure 33*a*). Based on Youngblood & Sottos (2008), coagulation and inflammation begin immediately when tissue is wounded. After approximately 24 hours, the cell proliferation and matrix deposition begin to close the wound. During the final stage of healing (which can take several days), the extracellular matrix is synthesized and remodelled as the tissue regains strength and function. Ideally, synthetic reproduction of the healing process in a material requires an initial rapid response to mitigate further damage, efficient transport of reactive materials to the damage site and structural regeneration to recover full performance.

Various self-healing artificial materials are being developed (Wool 2008; van der Zwaag *et al.* in press). In polymers and polymer composites, based on Youngblood & Sottos (2008), two approaches are being pursued. In the first approach, the crack-mending process is initiated by an external thermal-, photo-, mechanical- or chemical-induced stimulus. Crack healing is achieved through both molecular diffusion and thermally reversible solid-state reactions. In the second approach, damage, in the form of a crack, triggers the release of the healing agents stored in the material, as also occurs for fracture events in biological systems (figure 33*b*).

(*m*) *Sensory-aid devices*

Animals and humans can hear or detect sound or noise by detecting frequency domains. They use a basilar membrane that separates sounds according to their frequency, which are then conducted to the sensory cells (hair cells) that transform the vibration of the basilar membrane into a neural code (Moller 2006). Various nanostructures are being developed for frequency detection and sound imaging (Barth *et al.* 2003; Bar-Cohen 2006).

An array of sensors can be used to analyse chemicals and can lead to an 'artificial nose' for sense of smell or an 'artificial tongue' for sense of taste. Various techniques, such as atomic force microscope cantilever arrays, have been suggested for this purpose. Baller *et al.* (2000) used a microfabricated array of silicon cantilevers for the detection of vapours. Each of the cantilevers was coated with a specific sensor layer to transduce a physical process or a chemical reaction into a nanomechanical response. The response pattern of eight cantilevers was analysed with principal component analysis and artificial neural network techniques, which facilitates the application of the device as an artificial chemical nose. Single-cantilever sensors can determine quantities below the detection limits of equivalent 'classical' methods; thus, catalytic processes can be observed with picojoule sensitivity in nanocalorimetry (Gimzewski *et al.* 1994).

Melanophila beetle possess one infrared (IR) organ (containing 70 singly IR receptors) on each side of the thorax (Schmitz *et al.* 2007). Insect-inspired IR sensors are being developed for various applications, such as heat and smoke detection (Schuetz *et al.* 1999).

(*n*) *Other lessons from nature*

Human skin is sensitive to impact, leading to the purple colour marks in areas that are hit. This idea inspired researchers in the mid-1980s to develop a coating, indicating impact damage (Bar-Cohen 2006). Such a coating, on the basis of a paint mixed with microcapsules (1–10 μm in size) with a certain chemical reagent, was used in the aircraft industry to identify damage to components made of impact-sensitive composite materials. An impact may lead to a significant strength loss in such a material, without visible structural damage, so the change of colour indicates the damage that may be potentially dangerous for the aircraft.

Human body joints consist of softer cartilage between the two bones to reduce friction and wear. This concept is being used to develop artificial joints that involve ultrahigh molecular weight polyethylene. The sandfish found in the Sahara desert moves over the sand. The scales on its body and biomaterials used in the body provide wear resistance. This family of materials and the scales present on the body can be used to develop materials for abrasive wear resistance applications.

The pearl oyster uses carbon dioxide to construct its calcium carbonate shell. This technology is being exploited to convert carbon dioxide emissions into a water-based solution of bicarbonate ions, which can then be converted into solid calcium carbonate. The whale heart can pump of the order of 1000 l of blood per pulse through more than 170 km of veins and arteries. The construction of the whale heart is used as a model to develop pacemakers for high blood circulation.

Other lessons from nature include fly wings of flying insects, ultrasonic detection by bats and silent flying of owls. The latter occurs because of frayed feathers on the edges of their wings, which break up turbulence and reduce sound.

(*o*) *Hierarchical organization in biomaterials*

Nature develops biological objects by means of growth or biologically controlled self-assembly adapting to the environmental condition and by using the most commonly found materials. Biological materials are developed by using the recipes contained in the genetic code. As a result, biological materials and tissues are created by hierarchical structuring at all levels in order to adapt form and structure to the function, which have the capability of adaptation to changing conditions and self-healing (Fratzl & Weinkamer 2007; Nosonovsky & Bhushan 2008*a*). The genetic algorithm interacts with the environmental condition, which provides flexibility. For example, a tree branch can grow differently in the direction of the wind and in the opposite direction. The only way to provide this adaptive self-assembly is a hierarchical self-organization of the material. Hierarchical structuring allows adaptation and optimization of the material at each level.

It is apparent that nature uses hierarchical structures, consisting of nano-structures in many cases, to achieve the required performance (Nosonovsky & Bhushan 2008*a–c*). Understanding the role of hierarchical structure and development of low cost and flexible fabrication techniques would facilitate commercial applications.

3. Outlook

The emerging field of biomimetics is already gaining a foothold in the scientific and technical arena. It is clear that nature has evolved and optimized a large number of materials and structured surfaces with rather unique characteristics. As we understand the underlying mechanisms, we can begin to exploit them for commercial applications.

The commercial applications include new nanomaterials, nanodevices and processes. As for devices, these include superhydrophobic self-cleaning and/or low drag surfaces, surfaces for energy conversion and conservation, super-adhesives, robotics, objects that provide aerodynamic lift, materials and fibres with high mechanical strength, antireflective surfaces and surfaces with hues, artificial furs and textiles, various biomedical devices and implants, self-healing materials and sensory-aid devices, to name a few.

The author would like to sincerely thank Dr Kerstin Koch of the University of Bonn for useful suggestions and a critical reading of the paper.

References

Alberts, B., Johnson, A., Lewis, J., Raff, M., Roberts, K. & Walter, P. (eds) 2008 *Molecular biology of the cell*. New York, NY: Garland Science.

Alexander, R. M. & Diskin, A. 2004 *Human bones: a scientific and pictorial investigation*. New York, NY: Pi Press.

Anon. 2007 *Biomimetics: strategies for product design inspired by nature*. Bristol, UK: Department of Trade and Industry.

Arzt, E., Gorb, S. & Spolenak, R. 2003 From micro to nano contacts in biological attachment devices. *Proc. Natl Acad. Sci. USA* **100**, 10 603–10 606. (doi:10.1073/pnas.1534701100)

Autumn, K. 2006 How gecko toes stick. *Am. Sci.* **94**, 124–132. (doi:10.1511/2006.58.124)

Autumn, K., Liang, Y. A., Hsieh, S. T., Zesch, W., Chan, W. P., Kenny, T. W., Fearing, R. & Full, R. J. 2000 Adhesive force of a single gecko foot-hair. *Nature* **405**, 681–685. (doi:10.1038/35015073)

Ball, P. 2002 Natural strategies for the molecular engineer. *Nanotechnology* **13**, R15–R28. (doi:10.1088/0957-4484/13/5/201)

Baller, M. K. *et al.* 2000 A cantilever array-based artificial nose. *Ultramicroscopy* **82**, 1–9. (doi:10.1016/S0304-3991(99)00123-0)

Bar-Cohen, Y. (ed.) 2006 *Biomimetics: biologically inspired technologies*. Boca Raton, FL: Taylor & Francis.

Barnes, W. J. P., Smith, J., Oines, C. & Mundl, R. 2002 Bionics and wet grip. *Tire Technol. Int.* **2002**, 56–60.

Barth, F. G., Humphrey, J. A. C. & Secomb, T. W. 2003 *Sensors and sensing in biology and engineering*. New York, NY: Springer.

Barthelat, F., Tang, H., Zavattieri, P. D., Li, C. M. & Espinosa, H. D. 2007 On the mechanics of mother-of-pearl: a key feature in the material hierarchical structure. *J. Mech. Phys. Solids* **55**, 306–337. (doi:10.1016/j.jmps.2006.07.007)

Barthlott, W. & Neinhuis, C. 1997 Purity of the sacred lotus, of escape from contamination in biological surfaces. *Planta* **202**, 1–8. (doi:10.1007/s004250050096)

Baumann, M., Sakoske, G., Poth, L. & Tuenker, T. 2003 Learning from the lotus flower—self-cleaning coatings on glass. In *Proc. 8th Int. Glass Conf., Tampere, Finland*, pp. 330–333. Glass Processing Days.

Bechert, D. W., Bruse, M., Hage, W., van der Hoeven, J. G. T. & Hoppe, G. 1997 Experiments on drag-reducing surfaces and their optimization with an adjustable geometry. *J. Fluid Mech.* **338**, 59–87. (doi:10.1017/S0022112096004673)

Bechert, D. W., Bruse, M., Hage, W. & Meyer, R. 2000 Fluid mechanics of biological surfaces and their technological application. *Naturwissenschaften* **87**, 157–171. (doi:10.1007/s001140050696)

Benniston, A. C. & Harriman, A. 2008 Artificial photosynthesis. *Mater. Today* **11**, 26–34. (doi:10.1016/S1369-7021(08)70250-5)

Bhushan, B. 1999 *Principles and applications of tribology.* New York, NY: Wiley.

Bhushan, B. 2002 *Introduction to tribology.* New York, NY: Wiley.

Bhushan, B. 2007*a* *Springer handbook of nanotechnology*, 2nd edn. Heidelberg, Germany: Springer.

Bhushan, B. 2007*b* Adhesion of multi-level hierarchical attachment systems in gecko feet. *J. Adhes. Sci. Technol.* **21**, 1213–1258. (doi:10.1163/156856107782328353)

Bhushan, B. (ed.) 2008 *Nanotribology and nanomechanics: an introduction,* 2nd edn. Heidelberg, Germany: Springer.

Bhushan, B. & Jung, Y. C. 2006 Micro- and nanoscale characterization of hydrophobic and hydrophilic leave surface. *Nanotechnology* **17**, 2758–2772. (doi:10.1088/0957-4484/17/11/008)

Bhushan, B. & Jung, Y. C. 2008 Wetting, adhesion and friction of superhydrophobic and hydrophilic leaves and fabricated micro/nanopatterned surfaces. *J. Phys. Condens. Matter* **20**, 225 010. (doi:10.1088/0953-8984/20/22/225010)

Bhushan, B. & Ling, X. 2008 Integrating electrowetting into micromanipulation of liquid. *J. Phys. Condens. Matter* **20**, 485 009. (doi:10.1088/0953-8984/20/48/485009)

Bhushan, B. & Sayer, R. A. 2007 Surface characterization and friction of a bio-inspired reversible adhesive tape. *Microsyst. Technol.* **13**, 71–78. (doi:10.1007/s00542-006-0256-2)

Bhushan, B., Jung, Y. C. & Koch, K. In press. Micro-, nano-, and hierarchical structures for superhydrophobicity, self-cleaning and low adhesion. *Phil. Trans. R. Soc. A* **367**. (doi:10.1098/rsta.2009.0014)

Bormashenko, E., Bormashenko, Y., Stein, T., Whyman, G. & Bormashenko, E. 2007 Why do pigeon feathers repel water? Hydrophobicity of pennae, Cassie–Baxter wetting hypothesis and Cassie–Wenzel capillarity-induced wetting transition. *J. Colloid Interface Sci.* **311**, 212–216. (doi:10.1016/j.jcis.2007.02.049)

Clapham, P. B. & Hutley, M. C. 1973 Reduction of length reflection by moth eye principle. *Nature* **244**, 281–282. (doi:10.1038/244281a0)

Cutkosky, M. & Kim, S. In press. Design and fabrication of multi-material structures for bio-inspired robots. *Phil. Trans. R. Soc. A* **367**. (doi:10.1098/rsta.2009.0013)

Dendl, P. & Interwies, J. 2001 *Method for imparting a self-cleaning feature to a surface, and an object provided with a surface of this type.* German Patent no. WO 2001/079 141.

Dzenis, Y. 2004 Spinning continuous fibers for nanotechnology. *Science* **25**, 1917–1919. (doi:10.1126/science.1099074)

Elbaum, R., Gorb, S. & Fratzl, P. 2008 Structures in cell wall that enable hygroscopic movement of wheat awns. *J. Struct. Biol.* **164**, 101–107. (doi:10.1016/j.jsb.2008.06.008)

Fantner, G. E. *et al.* 2005 Sacrificial bonds and hidden length dissipate energy as mineralized fibrils separate during bone fracture. *Nat. Mater.* **4**, 612–616. (doi:10.1038/nmat1428)

Federle, W. 2006 Why are so many adhesive pads hairy? *J. Exp. Biol.* **209**, 2611–2621. (doi:10.1242/jeb.02323)

Federle, W., Barnes, W. J. P., Baumgartner, W., Drechsler, P. & Smith, J. M. 2006 Wet but not slippery: boundary friction in tree frog adhesive toe pads. *J. R. Soc. Interface* **3**, 689–697. (doi:10.1098/rsif.2006.0135)

Fish, F. E. 2006 Limits of nature and advances of technology: what does biomimetics have to offer to aquatic robots? *Appl. Bionics Biomech.* **3**, 49–60. (doi:10.1533/abbi.2004.0028)

Fish, F. E. & Battle, J. M. 1995 Hydrodynamic design of the humpback whale flipper. *J. Morphol.* **225**, 51–60. (doi:10.1002/jmor.1052250105)

Fratzl, P. 2008 Bone fracture—when cracks begin to show. *Nat. Mater.* **7**, 610–612. (doi:10.1038/nmat2240)

Fratzl, P. & Weinkamer, R. 2007 Nature's hierarchical materials. *Prog. Mater. Sci.* **52**, 1263–1334. (doi:10.1016/j.pmatsci.2007.06.001)

Fratzl, P., Elbaum, R. & Burgert, I. 2008 Cellulose fibrils direct plant organ movement. *Faraday Discuss.* **139**, 275–282. (doi:10.1039/b716663j)

Gao, X. F. & Jiang, L. 2004 Biophysics: water-repellent legs of water striders. *Nature* **432**, 36. (doi:10.1038/432036a)

Gao, L. & McCarthy, T. J. 2006 Artificial lotus leaf prepared using a 1945 patent and a commercial textile. *Langmuir* **22**, 5998–6000. (doi:10.1021/la061237x)

Gao, H., Wang, X., Yao, H., Gorb, S. & Arzt, E. 2005 Mechanics of hierarchical adhesion structures of geckos. *Mech. Mater.* **37**, 275–285. (doi:10.1016/j.mechmat.2004.03.008)

Gao, H., Liu, Z., Zhang, J., Zhang, G. & Xie, G. 2007*a* Precise replication of antireflective nanostructures from biotemplates. *Appl. Phys. Lett.* **90**, 123 115. (doi:10.1063/1.2715094)

Gao, X., Yan, X., Yao, X., Xu, L., Zhang, K., Zhang, J., Yang, B. & Jiang, L. 2007*b* The dry-style antifogging properties of mosquito compound eyes and artificial analogues prepared by soft lithography. *Adv. Mater.* **19**, 2213–2217. (doi:10.1002/adma.200601946)

Geim, A. K., Dubonos, S. V., Grigorieva, I. V., Novoselov, K. S., Zhukov, A. A. & Shapoval, S. Y. 2003 Microfabricated adhesive mimicking gecko foot-hair. *Nat. Mater.* **2**, 461–463. (doi:10.1038/nmat917)

Genzer, J. & Efimenko, K. 2006 Recent developments in superhydrophobic surfaces and their relevance to marine fouling: a review. *Biofouling* **22**, 339–360. (doi:10.1080/08927010600980223)

Gillmor, S. D., Thiel, A. J., Strother, T. C., Smith, L. M. & Lagally, M. G. 2000 Hydrophilic/hydrophobic patterned surfaces as templates for DNA arrays. *Langmuir* **16**, 7223–7228. (doi:10.1021/la991026a)

Gimzewski, J. K., Gerber, C., Meyer, E. & Schlittler, R. R. 1994 Observation of a chemical reaction using a micromechanical sensor. *Chem. Phys. Lett.* **217**, 589–594. (doi:10.1016/0009-2614(93)E1419-H)

Gorb, S. 2001 *Attachment devices of insect cuticle*. Dordrecht, The Netherlands: Kluwer Academic.

Gorb, S. 2006 Functional surfaces in biology: mechanisms and applications. In *Biomimetics: biologically inspired technologies* (ed. Y. Bar-Cohen), pp. 381–397. Boca Raton, FL: Taylor & Francis.

Gorb, E., Haas, K., Henrich, A., Enders, S., Barbakadze, N. & Gorb, S. 2005 Composite structure of the crystalline epicuticular wax layer of the slippery zone in the pitchers of the carnivorous plant *Nepenthes alata* and its effect on the insect attachment. *J. Exp. Biol.* **208**, 4651–4662. (doi:10.1242/jeb.01939)

Gorb, S., Varenberg, M., Peressadko, A. & Tuma, J. 2007 Biomimetic mushroom-shaped fibrillar adhesive microstructure. *J. R. Soc. Interface* **4**, 271–275. (doi:10.1098/rsif.2006.0164)

Gordon, J. E. 1976 *The new science of strong materials, or why you don't fall through the floor*, 2nd edn. London, UK: Pelican–Penguin.

Gosline, J., Nichols, C., Guerette, P., Chang, A. & Katz, S. 1995 The macromolecular design of spiders silks. In *Biomimetics: design and processing of materials* (eds M. Sarikaya & I. A. Aksay), pp. 237–261. Woodbury, NY: American Institute of Physics.

Goswami, L., Dunlop, J. W. C., Jungniki, K., Eder, M., Gierlinger, N., Coutand, C., Jeronimidis, G., Fratzl, P. & Burgert, I. 2008 Stress generation in the tension wood of poplar is based on the lateral swelling power of the G-layer. *Plant J.* **56**, 531–538. (doi:10.1111/j.1365-313X.2008.03617.x)

Grunwald, I., Rischka, K., Kast, S., Scheibel, T. & Bargel, H. In press. Mimicking biopolymers on a molecular scale: nano(bio)technology based on engineered proteins. *Phil. Trans. R. Soc. A* **367**. (doi:10.1098/rsta.2009.0012)

Hadobás, K., Kirsch, S., Carl, A., Acet, M. & Wasserman, E. F. 2000 Reflection properties of nanostructure-arrayed silicon surfaces. *Nanotechnology* **11**, 161–164. (doi:10.1088/0957-4484/11/3/304)

Hoecker, H. 2002 Plasma treatment of textile fibres. *Pure Appl. Chem.* **74**, 423–427. (doi:10.1351/pac200274030423)

Hoyt, J. W. 1975 Hydrodynamic drag reduction due to fish slimes. In *Swimming and flying in nature*, vol. 2 (eds T. Y. T. Wu, C. J. Brokaw & C. Brennen), pp. 653–672. New York, NY: Plenum.

Jackson, A. P., Vincent, J. F. V. & Turner, R. M. 1988 The mechanical design of nacre. *Proc. R. Soc. B* **234**, 415–440. (doi:10.1098/rspb.1988.0056)

Jakab, P. L. 1990 *Vision of a flying machine*. Washington, DC: Smithsonian Institution Press.

Jin, H.-J. & Kaplan, D. L. 2003 Mechanism of silk processing in insects and spiders. *Nature* **424**, 1057–1061. (doi:10.1038/nature01809)

Jones, C. J. & Aizawa, S. 1991 The bacterial flagellum and flagellar motor: structure, assembly, and functions. *Adv. Microb. Physiol.* **32**, 109–172. (doi:10.1016/S0065-2911(08)60007-7)

Juniper, B. E., Robins, R. J. & Joel, D. M. 1989 *The carnivorous plants*. London, UK: Academic Press.

Kertezs, K., Balint, Z., Vertesy, Z., Mark, G. I., Louse, V., Vigneron, J. P. & Biro, L. P. 2006 Photonic crystal type structures of biological origin: structural and spectral characterization. *Curr. Appl. Phys.* **6**, 252–258. (doi:10.1016/j.cap.2005.07.051)

Koch, K., Bhushan, B. & Barthlott, W. 2008 Diversity of structure, morphology, and wetting of plant surfaces. *Soft Matter* **4**, 1943–1963. (doi:10.1039/b804854a)

Koch, K., Bhushan, B. & Barthlott, W. 2009 Multifunctional surface structures of plants: an inspiration for biomimetics. *Prog. Mater. Sci.* **54**, 137–178. (doi:10.1016/j.pmatsci.2008.07.003)

Koch, K., Bhushan, B. & Barthlott, W. In press *a*. Functional plant surfaces, smart materials. In *Springer handbook of nanotechnology* (ed. B. Bhushan), 3rd edn. Heidelberg, Germany: Springer.

Koch, K., Bhushan, B., Jung, Y. C. & Barthlott, W. In press *b*. Fabrication of artificial lotus leaves and significance of hierarchical structure for superhydrophobicity and low adhesion. *Soft Matter*.

Koch, K., Bhushan, B., Ensikat, H.-J. & Barthlott, W. In press *c*. Self-healing of voids in the wax coating on plant surfaces. *Phil. Trans. R. Soc. A* **367**. (doi:10.1098/rsta.2009.0015)

Krink, T. & Vollrath, F. 1997 Spider web-building behavior with rule based simulation and genetic algorithms. *J. Theor. Biol.* **185**, 321–331. (doi:10.1006/jtbi.1996.0306)

Li, X. D., Change, W.-C., Chao, Y. J., Wang, R. Z. & Change, M. 2004 Nanoscale structural and mechanical characterization of a natural nanocomposite material: the shell of a red abalone. *Nano Lett.* **4**, 613–617. (doi:10.1021/nl049962k)

Lin, A. & Meyers, M. A. 2005 Growth and structure in abalone shells. *Mater. Sci. Eng. A* **390**, 27–41. (doi:10.1016/j.msea.2004.06.072)

Linde, A. & Goldberg, M. 1993 Dentinogenesis. *Crit. Rev. Oral. Biol. Med.* **4**, 679–728. (doi:10.1177/1045441/930040050301)

Lowenstam, H. A. & Weiner, S. 1989 *On biomineralization*. Oxford, UK: Oxford University Press.

Luz, G. M. & Mano, J. F. 2009 Biomimetic design of materials and biomaterials inspired by the structure of nacre. *Phil. Trans. R. Soc. A* **367**, 1587–1605. (doi:10.1098/rsta.2009.0007)

Mann, S. 2001 *Biomineralization*. Oxford, UK: Oxford University Press.

Meyers, M. A., Lin, A. Y. M., Seki, Y., Chen, P. Y., Kad, B. K. & Bodde, S. 2006 Structural biological composites: an overview. *JOM* **58**, 35–41. (doi:10.1007/s11837-006-0138-1)

Meyers, M. A., Chen, P. Y., Lin, A. Y. M. & Seki, Y. 2008 Biological materials: structure and mechanical properties. *Prog. Mater. Sci.* **53**, 1–206. (doi:10.1016/j.pmatsci.2007.05.002)

Milwich, M., Speck, T., Speck, O., Stegmaier, T. & Planck, H. 2006 Biomimetics and technical textiles: solving engineering problems with the help of nature's wisdom. *Am. J. Bot.* **93**, 1455–1465. (doi:10.3732/ajb.93.10.1455)

Moller, A. R. 2006 *Hearing: anatomy, physiology and disorders of the auditory systems*, 2nd edn. London, UK: Academic Press.

Motier, J. F. & Carrier, A. M. 1989 Recent studies on polymer drag reduction in commercial pipelines. In *Drag reduction in fluid flows: techniques for friction control* (eds R. H. J. Sellin & R. T. Moses). Chichester, UK: Ellis Horwood.

Mueller, T. 2008 Biomimetics design by natures. *National Geographic*, April 2008, pp. 68–90.

Mueller, F. & Winter, P. 2004 Clean surfaces with the lotus-effect. *Jornadas Comite Espanol de la Detergencia* **34**, 103–111.

Munch, E., Launey, M. E., Alsem, D. H., Saiz, E., Tomsia, A. P. & Ritchie, R. O. 2008 Tough bio-inspired hybrid materials. *Science* **322**, 1516–1520. (doi:10.1126/science.1164865)

Neinhuis, C. & Barthlott, W. 1997 Characterization and distribution of water-repellent, self-cleaning plant surfaces. *Ann. Bot.* **79**, 667–677. (doi:10.1006/anbo.1997.0400)

Nosonovsky, M. & Bhushan, B. 2008*a* *Multiscale dissipative mechanisms and hierarchical surfaces: friction, superhydrophobicity, and biomimetics*. Heidelberg, Germany: Springer.

Nosonovsky, M. & Bhushan, B. 2008*b* Roughness-induced superhydrophobicity: a way to design non-adhesive surfaces. *J. Phys. Condens. Matter* **20**, 225 009. (doi:10.1088/0953-8984/20/22/225009)

Nosonovsky, M. & Bhushan, B. 2008*c* Biologically-inspired surfaces: broadening the scope of roughness. *Adv. Funct. Mater.* **18**, 843–855. (doi:10.1002/adfm.200701195)

Nun, E., Oles, M. & Schleich, B. 2002 *Surfaces rendered self-cleaning by hydrophobic structures and a process for their production*. United States Patent no. 7211 313.

Ohler, A. 1995 Digital pad morphology in torrent-living ranid frogs. *Asiat. Herpetol. Res.* **6**, 85–96.

Parker, A. In press. Natural photonics for industrial inspiration. *Phil. Trans. R. Soc. A* **367**. (doi:10.1098/rsta.2009.0016)

Parker, A. R. & Lawrence, C. R. 2001 Water capture by a desert beetle. *Nature* **414**, 33–34. (doi:10.1038/35102108)

Reed, E. J., Klumb, L., Koobatian, M. & Viney, C. 2009 Biomimicry as a route to new materials: what kinds of lessons are useful? *Phil. Trans. R. Soc. A* **367**, 1571–1585. (doi:10.1098/rsta.2009.0010)

Reif, W. E. 1985 Squamation and ecology of sharks. *Courier Forschungsinstitut Senckenberg* **78**, 1–255. (Frankfurt am Main)

Roach, P., Shirtcliffe, N. J. & Newton, M. I. 2008 Progress in superhydrophobic surface development. *Soft Matter* **4**, 224–240. (doi:10.1039/b712575p)

Sarikaya, M. & Aksay, I. A. (eds) 1995 *Biomimetic design and processing of materials*. Woodbury, NY: American Institute of Physics.

Sarikaya, M. & Tamerler, C. In press. Molecular biomimetics: nanotechnology and bionanotechnology utilizing genetically engineered peptides. *Phil. Trans. R. Soc. A* **367**. (doi:10.1098/rsta.2009.0018)

Sarikaya, M., Gunnison, K. E., Yasrebi, M. & Aksay, I. A. 1990 Mechanical property–microstructural relationship in abalone shell. In *MRS Symp. Proc.*, vol. 174 (eds P. Rieke, P. D. Calvert & M. Alper), pp. 109–116. Pittsburgh, PA: Materials Research Society.

Schmitz, A., Sehrbrock, A. & Schmitz, H. 2007 The analysis of the mechanosensory origin of the infrared sensilla in *Melanophila acuminata* (Coeloptera; Buprestidae) adduces new insight into the transduction mechanism. *Arthropod Struct. Dev.* **36**, 291–303. (doi:10.1016/j.asd.2007.02.002)

Scholz, I., Barnes, W. J. P., Smith, J. M. & Baumgartner, W. 2009 Ultrastructure and physical properties of an adhesive surface, the toe pad epithelium of the tree frog, *Litoria caerulea* white. *J. Exp. Biol.* **212**, 155–162. (doi:10.1242/jeb.019232)

Schroeder, H. E. 1991 *Oral structural biology*. New York, NY: Thieme Medical Publications.

Schuetz, S., Weissbecker, B., Hummel, H. E., Apel, K.-H., Schmitz, H. & Bleckmann, H. 1999 Insect antennae as a smoke detector. *Nature* **398**, 298–299. (doi:10.1038/18585)

Sidorenko, A., Krupenkin, R., Taylor, A., Fratzl, P. & Aizenberg, J. 2007 Reversible switching of hydrogel-actuated nanostructures into complex micropatterns. *Science* **315**, 487–490. (doi:10.1126/science.1135516)

Singer, A. J. & Clark, R. A. F. 1999 Cutaneous wound healing. *N. Engl. J. Med.* **341**, 738–746. (doi:10.1056/NEJM199909023411006)

Stegmaier, T., Linke, M. & Planck, H. In press. Bionics in textiles: flexible and translucent thermal insulations for solar thermal applications. *Phil. Trans. R. Soc. A* **367**. (doi:10.1098/rsta.2009.0019)

Tang, Z., Kotov, N. A., Magonov, S. & Ozturk, B. 2003 Nanostructured artificial nacre. *Nat. Mater.* **2**, 413–418. (doi:10.1038/nmat906)

van der Zwaag, S., van Dijk, N., Jonkers, H., Mookhoek, S. & Sloof, W. In press. Self healing behaviour in man-made engineering materials: bio-inspired but tasking into account their intrinsic character. *Phil. Trans. R. Soc. A* **367**. (doi:10.1098/rsta.2009.0020)

Velcro, S. A. 1955 *Improvements in or relating to a method and a device for producing velvet type fabric*. Switzerland Patent no. 721 338.

Vincent, J. F. V., Bogatyreva, O. A., Bogatyrev, N. R., Bowyer, A. & Pahl, A. K. 2006 Biomimetics: its practice and theory. *J. R. Soc. Interface* **3**, 471–482. (doi:10.1098/rsif.2006.0127)

Vogel, S. 2003 *Comparative biomechanics: life's physical world*. Princeton, NJ: Princeton University Press.

Wagner, P., Furstner, R., Barthlott, W. & Neinhuis, C. 2003 Quantitative assessment to the structural basis of water repellency in natural and technical surfaces. *J. Exp. Bot.* **54**, 1295–1303. (doi:10.1093/jxb/erg127)

Wagner, G. J., Wang, E. & Shephers, R. W. 2004 New approaches for studying and exploiting an old protuberance, the plant trichome. *Ann. Bot.* **93**, 3–11. (doi:10.1093/aob/mch011)

Wang, R. Z., Addadi, L. & Weiner, S. 1997 Design strategies of sea urchin teeth: structure, composition, and micromechanical relations to function. *Phil. Trans. R. Soc. B* **352**, 469–480. (doi:10.1098/rstb.1997.0034)

Wang, R. Z., Suo, Z., Evans, A. G., Yao, N. & Aksay, I. A. 2001 Deformation mechanisms in nacre. *J. Mater. Res.* **16**, 2485–2493. (doi:10.1557/JMR.2001.0340)

Wang, S., Song, Y. & Jiang, L. 2007 Photoresponsive surfaces with controllable wettability. *J. Photochem. Photobiol. C: Photochem. Rev.* **8**, 18–29. (doi:10.1016/j.jphotochemrev.2007.03.001)

Wilson, S. J. & Hutley, M. C. 1982 The optical properties of the 'moth-eye' antireflective surfaces. *J. Modern Opt.* **29**, 993–1009. (doi:10.1080/713820946)

Wool, R. P. 2008 Self-healing materials: a review. *Soft Matter* **4**, 400–418. (doi:10.1039/b711716g)

Xia, F., Feng, L., Wang, S., Sun, T., Song, W., Jiang, W. & Jiang, L. 2006 Dual-responsive surfaces that switch between superhydrophilicity and superhydrophobicity. *Adv. Mater.* **18**, 432–436. (doi:10.1002/adma.200501772)

Youngblood, J. P. & Sottos, N. R. 2008 Bioinspired materials for self-cleaning and self-healing. *MRS Bull.* **33**, 732–738.

Zhai, L., Berg, M. C., Cebeci, F. C., Kim, Y., Milwild, J., Rubner, M. F. & Cohen, R. E. 2006 Patterned superhydrophobic surfaces: toward a synthetic mimic of the Namib desert beetle. *Nano Lett.* **6**, 1213–1217. (doi:10.1021/nl060644q)